GENERAL RESERCH PROFILE REPORT

ASSOCIATION OF TGF-β AND LACTATE IN THE INDUCTION OF REGULATORY T CELLS BY MESENCHYMAL-CRC ORGANOIDS

TESSA VREMAN (6270565)

Molecular and Cellular Life Sciences

Graduate School of Life Sciences

Utrecht University

Coffer lab, CMM & RMCU

EXAMINER: Prof. Dr. Paul Coffer

SECOND REVIEWER: Dr. Hugo Snippert

SUPERVISOR: Sonia Arístin Revilla

GRAPHICAL ABSTRACT

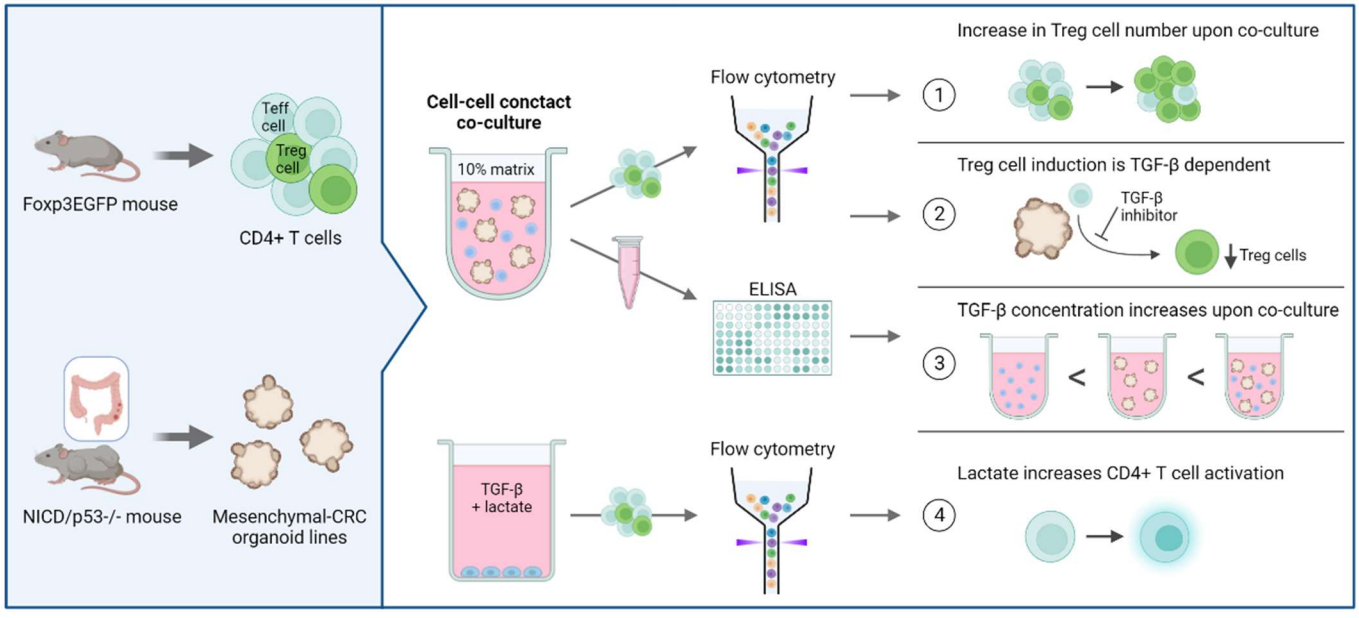

March 2023

ABSTRACT

Regulatory T cells (Treg cells) are a specialized subset of CD4+ T cells with an important role in immune regulation and disease pathogenesis. Treg cells can have an unfavorable effect in the context of cancer by suppressing anti-tumor immune responses. In CRC tumors, Treg cell enrichment correlates with tumor progression and metastasis, immunotherapy failure, and poor prognosis. In this study, we established cell-cell contact co-cultures with murine mesenchymal-CRC organoid lines and CD4+ T cells from Foxp3EGFP mice to explore the mechanisms underlying Treg cell enrichment in mesenchymal CRC. We analyzed the effect of two mesenchymal-CRC organoid lines on CD4+ T cell activation and Treg cell induction by flow cytometry. Our findings showed that mesenchymal-CRC organoid lines induce Treg cells in a transforming growth factor β (TGF-β)-dependent manner when co-cultured with CD4+ T cells. Furthermore, we studied the effect of TGF-β and lactate on the induction of Treg cells by culturing CD4+ T cells in low and high concentrations of TGF-β with or without lactate. We demonstrated that lactate enhanced CD4+ T cell activation but not Treg cell induction in conditions with low and high TGF-β concentrations. Overall, we developed an *in vitro* model with mesenchymal-CRC organoid lines and CD4+ T cells in which Treg cells are induced in a TGF-β-dependent manner. This Treg cell induction mimics to some extent the Treg cell enrichment in mesenchymal-CRC tumors described in literature. Thus, this co-culture model may help us study Treg cells in the context of mesenchymal CRC.

TABLE OF CONTENTS

LAYMAN'S SUMMARY

Colorectal cancer (CRC) is one of the leading causes of cancer-related deaths worldwide. Despite advances in treatment, the prognosis for patients diagnosed with advanced stages of CRC remains poor. It is important to gain a better understanding of CRC tumors because that is crucial in developing better treatment. Tumors are not only made up of tumor cells but also of immune cells. Immune cells are part of the immune system and, in general, protect the body against diseases. However, in CRC tumors, there are regulatory immune cells present that protect the tumor against the other immune cells. Regulatory immune cells are a type of immune cell that prevent an overreaction of the immune system to avoid autoimmune responses. The regulatory immune cells in CRC tumors block the immune system's ability to fight against the tumor. Thus, CRC patients have a worse prognosis when there are many regulatory immune cells present in the CRC tumor. In our research, we aimed to gain a better understanding of the regulatory immune cells in CRC tumors.

To study the regulatory immune cells in CRC tumors, we developed organoids from CRC tumors. An organoid is a microscopic version of a tumor with similar characteristics to the original tumor. We grew these CRC organoids together with immune cells, we call this setup a co-culture. The co-culture allows us to study the effect of the organoids on immune cells. We found that the CRC organoids caused an increase in the amount of regulatory immune cells, similar to what happens in CRC tumors in the human body. This suggests that the developed co-culture model can be used to study the regulatory immune cells in the context of CRC tumors. Furthermore, we added a chemical compound to the co-culture that is known to target the development of the regulatory immune cells. This compound suppressed the increase in the amount of regulatory immune cells by the CRC organoids. Altogether, these experiments showed that this model with CRC organoids and immune cells to some extent mimics the real-life tumor situation. Thus, this model can help us gain more insight into CRC tumors.

In order to use this model with CRC organoids to study regulatory immune cells in CRC tumors, it is necessary to further validate the model and prove that it is close to the real-life situation. It is also important to note that mice were used for the experiments in this study. Therefore, it is still necessary to conduct further studies with human material to determine the relevance of this model to human CRC tumors. Nevertheless, this study is an important step toward gaining a better understanding of the regulatory immune cells in CRC tumors.

INTRODUCTION

Regulatory T cells (Treg cells) are a subpopulation of CD4+ T cells that regulate the immune response (1). The concept of a subpopulation of T cells with a regulating function was introduced in the 1970s, this population was later defined in mice as 10% of CD4+ T cells expressing the interleukin-2 (IL-2) receptor alpha-chain (CD25) (2). However, the definition of 10% of CD4+CD25+ T cells was not specific enough since CD25 is a general marker for activation in T cells. More recently, the forkhead box P3 transcription factor (Foxp3) was found to be specifically expressed in CD4+CD25+ Treg cells. FOXP3 is essential for the differentiation, development, and function of Treg cells (3,4). Thus, Treg cells are now commonly defined as CD4+CD25+FOXP3+ T cells. Treg cells have multiple roles in regulating immune homeostasis, such as ensuring tolerance against autoantigens, commensal microflora antigens, and food antigens, they prevent an excessive immune response and regulate fetoplacental immunity (5–7).

Treg cell origin and differentiation

Treg cells can originate in two different ways: in the thymus (tTreg cells) from thymocytes and in the periphery (pTreg cells) from effector CD4+ (eCD4+) T cells (Figure 1A) (8). In the thymus, thymocytes with a TCR with high affinity for self-peptides start expressing *FOXP3* and differentiate into tTreg cells. tTreg cells are important in suppressing autoimmunity because they express TCRs that mainly recognize autoantigens. tTreg cells first reside in the lymphoid tissue as naïve Treg (nTreg) cells. nTreg cells can later be activated and migrate to peripheral tissues to become effector Treg (eTreg) cells which develop tissue-specific functions. This activation is mediated by the stimulation of the TCR by an antigen presented by MHC class II on an antigen-presenting cell (APC). Furthermore, complementary signals CD3 and CD28 are needed for activation. CD3 is a cell-surface receptor associated with the TCR, while CD28 is the receptor for CD80 and CD86 which are expressed by APCs. pTreg cells can differentiate from eCD4+ T cells through signaling by the main cytokines for Treg cell differentiation transforming growth factor β (TGF-β) and IL-2, supported by stimulation of the TCR (9,10). IL-2 promotes the activation of CD4+ T cells by binding to CD25 and TGF-β induces *FOXP3* expression. pTreg cells express TCRs that recognize foreign antigens, hence pTreg cells are important in tolerance to foreign antigens. Treg cells a have diverse TCR repertoire because of their thymic or peripheral origin which enables them to regulate the immune response to autoantigens and foreign antigens (11). In conclusion, tTreg cells originate in the thymus and have TCRs with affinity for autoantigens whereas pTreg cells originate in the periphery and have TCRs with affinity for foreign antigens.

TGF-β signaling drives the differentiation of Treg cells through the Smad signaling pathway (Figure 1B) (12). This pathway is activated by the binding of TGF-β to the heterodimer of two isoforms of the TGF-β receptor (TGFβR1 and TGFβR2) on the cell surface. Upon binding, TGFβR2 phosphorylates and activates TGFβR1. Activated TGFβR1 phosphorylates Smad2 and Smad3 which form a complex with Smad4 that relocates to the nucleus and promotes *FOXP3* expression. The expression of *FOXP3* is regulated by epigenetic changes in its promoter and enhancers, known as conserved non-coding sequences (CNS) 0-3 (13). The Smad2/3-Smad4 complex binds to CNS1, which leads to histone acetylation and enhancer activation, which drives the expression of *FOXP3*. Thus, the promotion of *FOXP3* expression by TGF-β signaling through the Smad pathway is crucial for the differentiation and function of Treg cells.

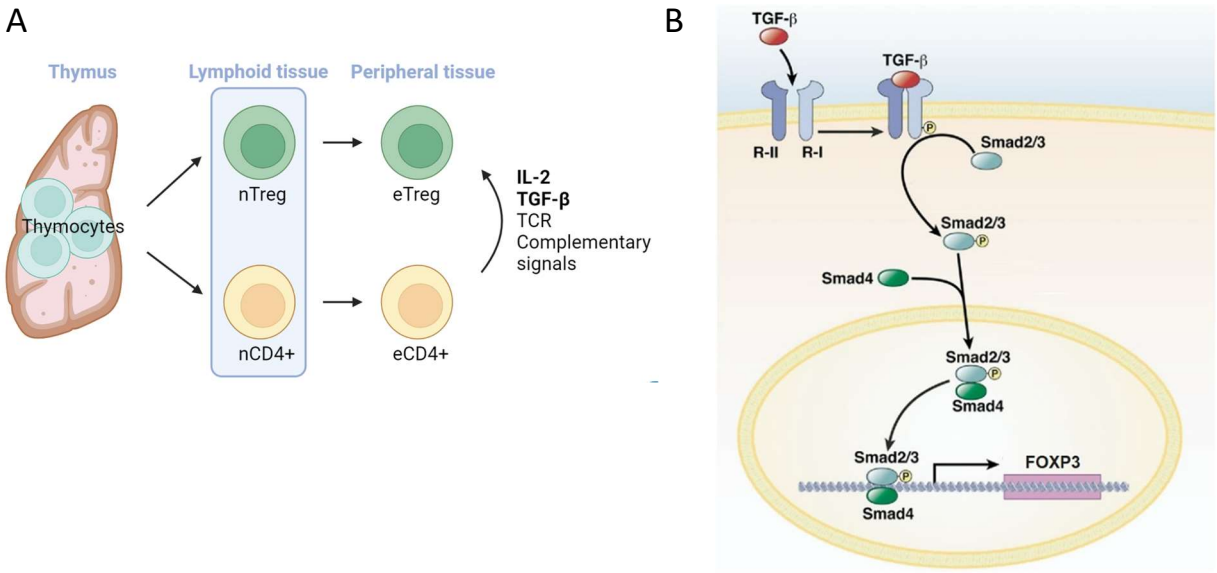

Figure 1 | Treg cell differentiation. **(A)** Treg cells can originate in two different ways: directly from thymocytes (tTreg cells) or from the conversion of effector CD4+ T cells in the periphery (pTreg cells) under the influence of IL-2, TGF-β, TCR signaling, and complementary signals. **(B)** TGF-β induces the transcription of *FOXP3* through Smad proteins (12).

Treg cell function in the TME of CRC

The main function of Treg cells is to suppress the immune response by inhibiting other immune cells like lymphocytes, macrophages, and APCs (14). The importance of Treg cells in maintaining immune homeostasis is highlighted by the development of lethal autoimmune diseases when Treg cells are depleted in FOXP3-mutant mice (3,15). However, besides the valuable role of Treg cells in regulating the immune response, they can also have an unfavorable effect by preventing anti-tumor immune response. This immune suppression by Treg cells occurs in colorectal cancer (CRC) tumors (16).

Treg cells perform their immunosuppressive function by using mechanisms such as inhibitory cytokines, cytolysis, metabolic disruption, and inhibiting maturation and function of APCs (17). The cytokines interleukin-10 (IL-10), IL-35, and TGF-β secreted by the Treg cells are inhibitory cytokines to inhibit effector T (Teff) cells, natural killer cells (NKs), and APCs. TGF-β can also be membrane-bound which mediates inhibition in a cell-contact-dependent manner (18). Additionally, Treg cells secrete granzymes and perforin which kill Teff cells, APCs, and B cells via cytolysis (19,20). Furthermore, Treg cells can metabolically disturb Teff cells by highly expressing CD25 and depleting the local environment of IL-2 so it is not available for Teff cells that need it to survive (21). Also, Treg cells inhibit Teff cells by exploiting the adenosine signaling pathway in Teff cells by secreting adenosine (22). Teff cells express the A2A receptor to be able to sense extracellular adenosine because of tissue damage caused by their immune response (23). Signaling of the A2A receptor in Teff cells results in a downregulation of their immune response. Instead of inhibiting Teff cells directly, Treg cells can also indirectly inhibit the immune response by modifying APC maturation and function via immune checkpoint receptors (24). APCs are essential for the activation of T cells (25). Treg cells can prevent APCs from activating T cells via several checkpoint receptors such as cytotoxic T-lymphocyte antigen 4 (CTLA-4) (26). Altogether, Treg cells can inhibit other immune cells through various mechanisms to perform their immunosuppressive function.

In addition, Treg cells affect the TME of CRC tumors by stimulating cancer-associated fibroblasts (CAFs) and angiogenesis (27). Treg cells secrete TGF-β which induces the conversion of fibroblasts to CAFs. CAFs are thought to play a critical role in tumor progression by producing extracellular matrix (ECM) proteins that create a stiff microenvironment that promotes the proliferation, invasion, and metastasis of cancer cells. This dense environment also prevents other immune cells from reaching the TME and killing tumor cells (28). Moreover, Treg cells produce vascular endothelial growth factor (VEGF) which promotes angiogenesis. Angiogenesis benefits tumor growth by providing sustenance and waste disposal (29). In summary, Treg cells suppress the anti-tumor immune response and affect the TME of CRC tumors to benefit tumor growth and progression.

Mesenchymal CRC subtype

CRC is the third most diagnosed and second most mortal cancer type (30). Approximately 30% of all CRC cases are familial but only in about 5% of all cases, the cancer arises from a well-defined inherited syndrome (31). The other 70% of CRC cases are sporadic. 90% of patients that are diagnosed with early-stage CRC are still alive five years after they were first diagnosed. At an early stage, when the tumor is not metastasized, CRC is easier to treat by removing the tumor in surgery (32). However, CRC commonly metastasizes to the liver and lungs. When CRC is diagnosed in a later, metastatic stage, the five-year survival rate decreases to 14% (33,34). To improve possible treatment, the immune component of the TME of CRC must be better understood.

CRC is a heterogeneous disease subdivided into four consensus molecular subtypes (CMS1-4). The four subtypes differ in genetic, epigenomic, transcriptomic, tumor microenvironmental, prognostic, and clinical characteristics (35). Determining the subtype of CRC in patients can help improve prognostication and find suitable treatment strategies. One of the factors that differentiates the four CMS is their immune environment. Immune cells are a common part of the tumor microenvironment (TME) and they affect the development of the tumor (36). The type of immune cells and their response determine the effect on tumor growth and progression (37). Regarding the immune compartment of CRC tumors, CMS1 has an active immune response where CD4+ Teff cells, CD8+ Teff cells, NKs, and APCs are present. CMS2 and 3 have low immune infiltration by inactive immune cells. In contrast, the TME of CMS4 is pro-inflammatory and immunosuppressive cells such as Treg cells, myeloid-derived suppressor cells (MDSCs), and tumor-associated macrophages (TAMs) predominate. In part because of the immunosuppressive TME, CMS4 tumors have the worst prognosis and survival rate of the four CMS (35).

CMS4 is the mesenchymal subtype. Mesenchymal-CRC tumors are often diagnosed at advanced stages when the tumor is metastasized, which complicates treatment (38). Several treatments that show an effect on other types of cancer do not have the same effect on mesenchymal-CRC tumors. Adjuvant therapy is often used to reduce the risk of recurrence in patients but mesenchymal-CRC patients do not show any benefit from adjuvant treatments (39). For instance, anti-epidermal growth factor receptor (EGFR) therapies have beneficial effects on a variety of tumors (40). Anti-EGFR therapies inhibit the EGFR pathway via different mechanisms such as preventing ligand binding or inhibiting downstream effects of the ligand binding. However, mesenchymal-CRC tumors react poorly to anti-EGFR therapy. Another example of treatment is against angiogenesis using an antibody against vascular endothelial growth factor (VEGF). VEGF is a key factor in tumor angiogenesis and targeting VEGF prevents tumor growth (41). However, treatment with anti-VEGF antibodies only has limited beneficial effect on mesenchymal-CRC patients (42). In sum, the limited effective treatment options for mesenchymal CRC makes it crucial to find new treatments. Targeting the tumor-promoting Treg cells present in the TME could be a new and helpful addition to existing treatment because they prevent an anti-tumor immune response.

Treg cell enrichment in the TME of mesenchymal CRC

The tumor microenvironment (TME) of mesenchymal-CRC tumors is a complex environment composed of tumor cells, immune cells, stromal cells, endothelial cells, and extracellular matrix (ECM) (Figure 2A). Among the different immune cells, there are Teff cells, TAMs, MDSCs, and Treg cells. Treg cells are enriched in mesenchymal-CRC tumors and a high number of Treg cells in the TME is indicative of a poor prognosis (43,44).

The enrichment of Treg cells in the TME of mesenchymal-CRC tumors can be explained by several factors. One factor is that TGF-β is highly available in the TME of mesenchymal-CRC tumors. TGF-β signaling plays a role in the epithelial-to-mesenchymal transition of tumors (45). The availability of TGF-β stimulates Treg cell differentiation and function by stimulating *FOXP3* expression in CD4+ T cells in the TME. Thus, the presence of TGF-β promotes Treg cell accumulation in the TME of mesenchymal-CRC tumors. Another factor that promotes Treg cell enrichment in the TME involves the altered metabolism of tumor cells. Tumor cells do not metabolize glucose via the citric acid cycle but only partially digested glucose with lactate as an end product. Thus, the TME is a low glucose and high lactate environment. High lactate concentration influences the environment making it more acidic (46). Immune cells such as Teff cells cannot survive in the high lactate condition but Treg cells are metabolically flexible and can rely on lactate for their energy supply and survive in this environment (Figure 2B). Treg cells in the TME reduce their uptake of glucose and increase their uptake of lactate and fatty acids. This metabolic switch upregulates the TCA cycle and OXPHOS to adapt to the TME (47). To enable this switch to lactate metabolism, Treg cells upregulate their monocarboxylate transporters (MCT) to increase lactate uptake. Lactate Dehydrogenase A (LDHA), which catalyzes the conversion of lactate to pyruvate, is also upregulated (48). The pyruvate produced by LDHA is further used in the metabolic pathway. The metabolic flexibility of the Treg cells not only allows them to survive and proliferate, but lactate metabolism also increases their suppressive function (49). Furthermore, mesenchymal-CRC tumors express CC chemokines that recruit Treg cells to the TME (50). CC chemokines are a subtype of chemokines that share the same N-terminal CC domain and they are important in the recruitment of immune cells (51). Treg cells express CCR7 and CCR9 which are chemokine receptors that enable Treg cells to migrate to the tumor (52,53). CCR7 is especially

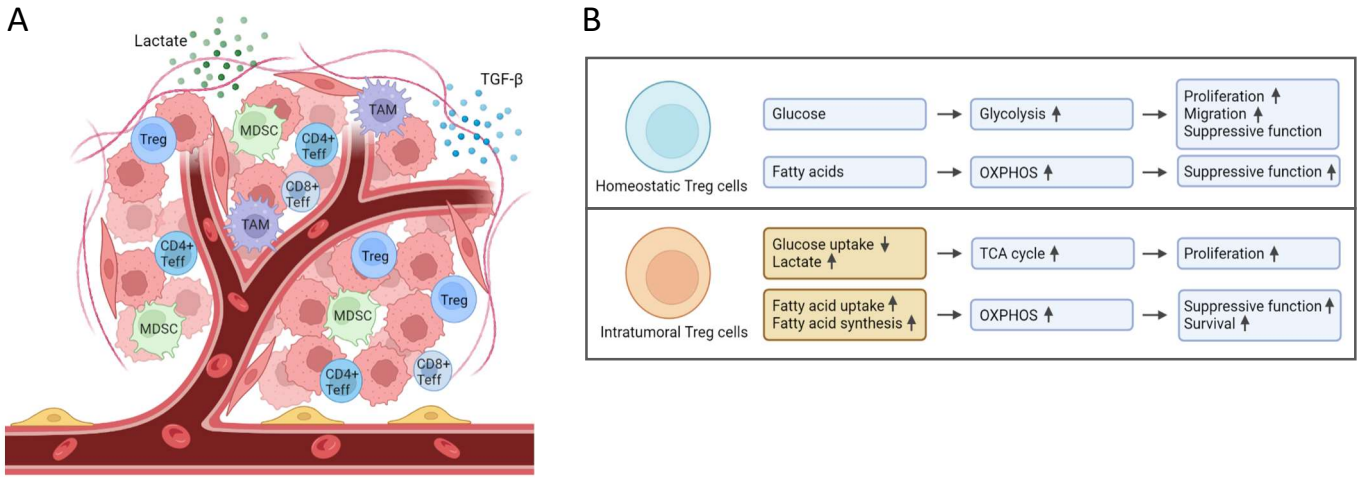

Figure 2 | Treg cell enrichment in the TME of mesenchymal-CRC tumors. **(A)** The TME of mesenchymal-CRC tumors is comprised of different cell types and structures like tumor cells, immune cells, stromal cells, endothelial cells, blood vessels, and extracellular matrix (ECM). Furthermore, it is characterized by having high lactate and TGF-β concentration. **(B)** Treg cells can switch their metabolism to use lactate instead of glucose as the main source of energy in a TME with high lactate concentration. The switch to lactate metabolism in Treg cells not only enables them to survive in the TME but also increases their immunosuppressive function (47).

highly expressed by nTreg cells, which lose that expression when they become eTreg cells (54). Altogether, several factors such as TGF-β availability, high lactate concentration, and chemokines are involved in Treg cell enrichment in the TME of mesenchymal-CRC tumors.

The tumor-promoting nature of Treg cells makes them an interesting target for therapies. However, the focus should be on only targeting the Treg cells in the tumor and not the natural Treg cells. Depleting natural Treg cells leads to disruption of immune homeostasis and unwanted side effects such as autoimmune diseases (3,15). Therefore, discerning the difference between Treg cells in the tumor and the natural Treg cells is essential for potential therapy development. This study aims to reveal the mechanisms involved in the induction of Treg cells from CD4+ T cells in the TME of mesenchymal CRC. To this end, we used co-cultures of murine CD4+ T cells and mesenchymal-CRC organoid lines. Murine Treg cells constitutively express *FOXP3* whereas human Treg cells have a more unstable *FOXP3* expression which complicates analysis. Firstly, we investigated the role of TGF-β in the induction of Treg cells by mesenchymal-CRC organoid lines. Later, we studied the effect of lactate on the activation and differentiation of Treg cells in different concentrations of TGF-β. In these experiments, we used flow cytometry to analyze CD4+ T cell activation and Treg cell differentiation. In this way, we studied the association of TGF-β and lactate in the induction of Treg cells by mesenchymal-CRC organoid lines.

MATERIALS AND METHODS

Solutions

- MACS buffer: PBS containing 2% FBS and 0.4% EDTA

Culture media

- BM2- medium: Advanced DMEM/F12, 2mM GlutaMax, 10mM HEPES, 50 U/ml Penicillin-Streptomycin
- BM2mouse (BM2m) medium: Advanced DMEM/F12, 2mM GlutaMax, 10mM HEPES, 50 U/ml Penicillin-Streptomycin, 100 ng/ml Noggin conditioned medium, 10nM Recombinant Murine FGF-basic, 1 mM N-Acetylcysteine, and B-27™ Supplement
- T cell medium (TCM): RPMI 1640 Medium, GlutaMax, 10% FBS, 1% Penicillin–Streptomycin
- Enriched T cell medium (eTCM): RPMI 1640 Medium, GlutaMax, 10% FBS, 1% Penicillin–Streptomycin, 1mM Sodium pyruvate, 1X Nonessential amino acids, 10mM HEPES, 50uM 2-Mercaptoethanol

Murine mesenchymal-CRC organoid culture

Transgenic C57BL/6 mice with conditionally activated Notch1 receptor and deleted p53 in the digestive epithelium (NICD/p53-/-) were generated by Chanrion et al. (55). These mice develop metastatic tumors in the digestive system characterized as mesenchymal-CRC tumors. Two organoid lines, bTL1 and dTSC1, were created from the tumors of these mice (Figure 3). dTSC1 and bTL1 organoid lines are cultured in droplets of 50% BME, as extracellular matrix, diluted in BM2- medium. When plating, the organoids in matrix were incubated at 37˚C for 30 minutes to allow the matrix to solidify. The plate was placed upside down during the incubation to distribute the organoids in the droplet. After the matrix was solidified, BM2mouse (BM2m) medium was added. Medium was refreshed after 4 days. After 7 days, organoid lines were passaged by making a single cell suspension with pre-warmed TrypLE™ Express Enzyme incubated for 7 minutes. During incubation with TrypLE™ Express Enzyme, the suspension was mechanically disrupted after 5 and 7 minutes. Then, the organoid lines were washed by adding PBS and centrifuged (1800rpm, 3 minutes). The organoid lines were usually passaged with a split ratio of 1:25.

alamarBlue viability assay with mesenchymal-CRC organoid lines

An alamarBlue viability assay was done to analyze the viability of dTSC1 and bTL1 organoid lines in different matrices. Organoid lines were cultured in a flat bottom 96-well cell culture plate in 10 and 50% BME or Matrigel and 0.25 and 0.5% GrowDex as extracellular matrix. The matrices were diluted in BM2m medium. 4 days after plating, 20 µl of alamarBlue was added to each well. After adding alamarBlue, the plate was put on a shaker for 15 minutes (protected from light) to distribute alamarBlue through the matrix. After 15 minutes, the plate was removed from the shaker and incubated for 3 hours at 37˚C protected from light. Then, 100 µl medium was removed from each well before the fluorescence was measured. The fluorescence (excitation 530-560 nm and emission 590 nm) was measured with a BMG LABTECH CLARIOstar® Plus multi-mode plate reader.

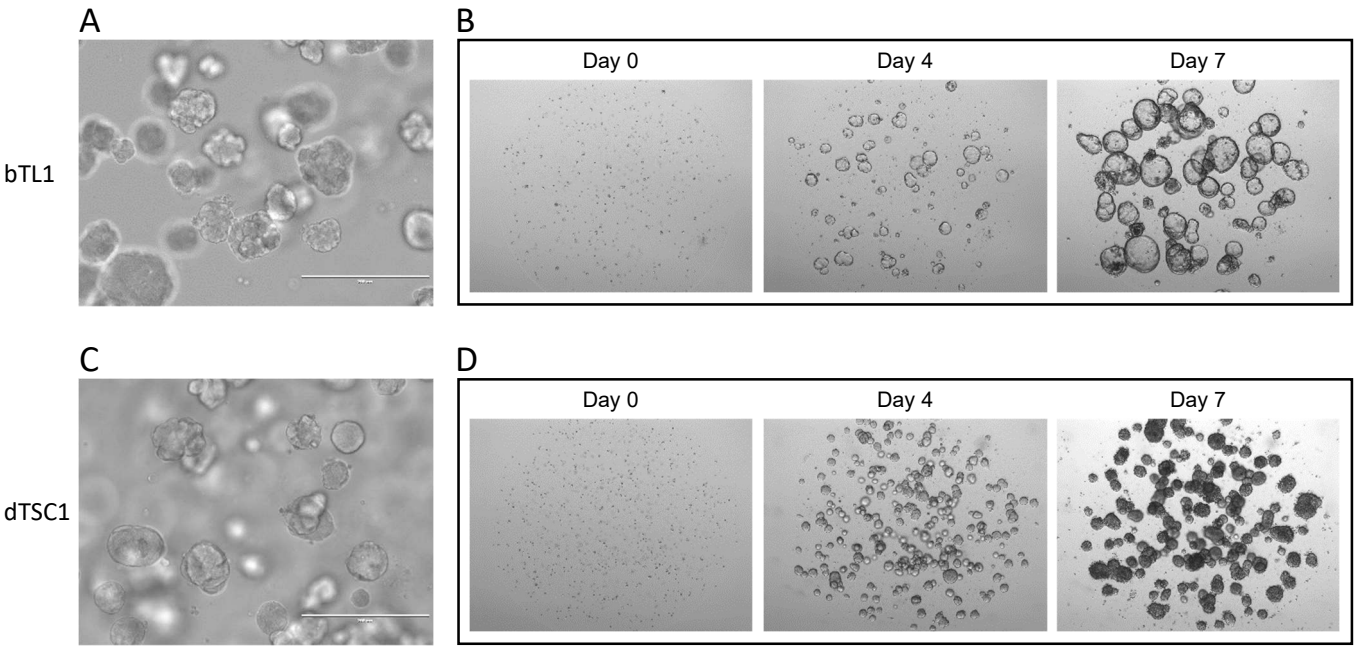

Figure 3 | bTL1 and dTSC1 organoid lines and their growth over 7 days. **(A)** bTL1 organoid line on day 4 after splitting at passage 24 at 20x magnification. The scale bar represents 200 µm. **(B)** Growth of bTL1 organoid line at passage 34 on the day of splitting (day 0), 4, and 7 days after splitting at 5x magnification. **(C)** dTSC1 organoid line on day 4 after splitting at passage 24 at 20x magnification. The scale bar represents 200 µm. **(D)** Growth of dTSC1 organoid line at passage 32 on the day of splitting (day 0), 4, and 7 days after splitting at 5x magnification. All images were captured on a brightfield microscope.

Murine CD4+ T cell isolation

For CD4+ T cell isolation, the inguinal, axillary, and cervical lymph nodes and spleen were collected from C57BL/6 Foxp3EGFP mice. These mice co-express EGFP and Foxp3 under the control of the Foxp3 promoter (56,57). The collected organs were smashed against a 70 µm cell strainer in T cell medium (TCM). Cells were resuspended in MACS buffer and counted using Trypan blue (1:2) with the Bio-Rad TC20 Automated Cell Counter. The total cell suspension was resuspended in 90 µl of MACS buffer per 10^7 total cells (with a minimum of 2.25 ml). Then, 10 µl of CD4 (L3T4) MicroBeads per 10^7 total cells was added (with a minimum of 250 µl). Cells and MicroBeads were incubated for 15 minutes at room temperature. Subsequently, cells were washed by adding MACS buffer and centrifuged (400g, 4 minutes, 4°C). Cells with MicroBeads were resuspended in 1 ml of MACS buffer and put on a pre-wetted LS column in the MACS Magnetic Separator. Then, the column was washed three times with 3 ml MACS buffer. To collect the CD4+ fraction, the column was removed from the MACS Magnetic Separator and CD4+ T cells were eluted with two times 5 ml MACS buffer. First, 5 ml MACS buffer was allowed to flow through the LS columns. The second time 5 ml MACS buffer was added, it was flushed through the LS column with a plunger. After isolation, CD4+ T cells were counted using Trypan blue (1:2) with the Bio-Rad TC20 Automated Cell Counter. The purity of the CD4+ T cell isolation was analyzed with flow cytometry (Figure 4).

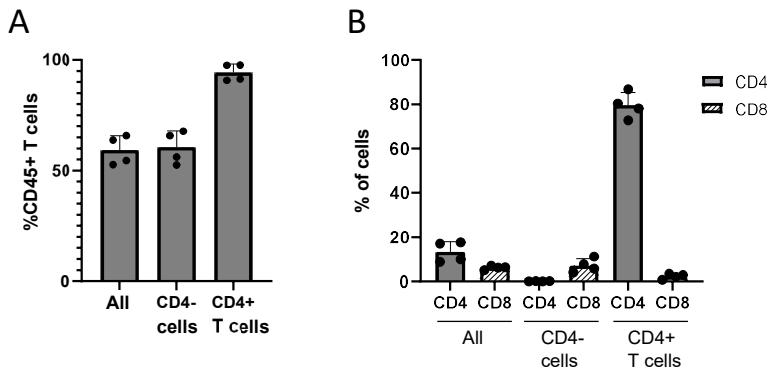

Figure 4 | Purity assessment of the murine CD4+ T cell isolation. Three cell fractions were analyzed using flow cytometry: cells collected from the lymph nodes and spleen before isolation (all), the negative fraction after isolation (CD4- cells), and the positive fraction after isolation (CD4+ T cells). **(A)** Percentage of CD45+ T cells in the three cell fractions. **(B)** Percentage of CD4+ and CD8+ T cells in the three cell fractions. Data represented as means ± SD. (n=3).

CD4+ T cell activation and induction of Treg cells *in vitro*

Murine CD4+ T cells were plated for experiments in a flat bottom 96-well cell culture plate resuspended in enriched T cell medium (eTCM). For experiments in which CD4+ T cells were plated in matrix, a U-bottom 96-well plate was used. To activate CD4+ T cells, cells were plated in eTCM or BM2m medium supplemented with anti-mouse CD3e monoclonal antibody (mAb), 1 µg/ml anti-mouse CD28 mAb, and 20 U/ml Recombinant Human IL-2 Protein. Anti-mouse CD3e mAb was added either in suspension (1 µg/ml) or coated on the plate. The plate was coated by washing the plate with PBS and incubating 50 µl of anti-mouse CD3e mAb (1 µg/ml) in PBS on the 96-well plate at 37°C for 3 hours. After incubation, the PBS with anti-mouse CD3e mAb was removed from the wells before plating the cells. For the induction of Treg cells, 300 U/ml Recombinant Human IL-2 Protein and Recombinant Human TGF-beta 1 in different concentrations (0.1, 1, 2, 5, or 10 ng/ml) were added. 200,000 CD4+ T cells were plated per well in a 96-well plate.

Co-culture systems with mesenchymal-CRC organoid lines and CD4+ T cells

To establish co-cultures, murine mesenchymal-CRC organoid lines (bTL1 and dTSC1) and CD4+ T cells were cultured together embedded in 10% BME or Matrigel diluted in BM2m medium in a U-bottom 96-well plate. 200,000 CD4+ T cells and 12,500 organoids were plated per well. To activate CD4+ T cells, 10% matrix diluted in BM2m medium was supplemented with anti-mouse CD3e mAb, 1 µg/ml anti-mouse CD28 mAb, and 20 U/ml Recombinant Human IL-2 Protein. Organoid lines were collected for co-culture on day 2 after splitting using dispase. Dispase was removed by washing twice with PBS and centrifuging (1800rpm, 3 minutes). The organoid pellet was resuspended in 1 ml BM2- medium. To count the organoids, a 1:100 dilution was made and three 3 µl droplets from this dilution were taken. The number of organoids per droplet was counted by eye using a brightfield microscope. To get the total amount of organoids, the average amount of organoids per droplet was used in the following formula:

$$total\ amount\ of\ organoids = \frac{average\ per\ droplet}{3} * 100 * 1000$$

Stainings and flow cytometry

Flow cytometry was used to analyze murine CD4+ T cells after culturing under different conditions. CD4+ T cells cultured in medium were collected by centrifuging (400g, 4 minutes, 4˚C) and washing with cold PBS (cPBS). CD4+ T cells cultured in matrix were collected by adding 150 µl cell recovery solution and incubating at 4˚C for 30 minutes and then washed with cPBS. CD4+ T cells cultured in GrowDex were collected by adding 40 µl GrowDase and incubating for 3 hours at 37 ˚C and then washed with cPBS. After collection, CD4+ T cells were stained with the dead/live dye Zombie NIR and surface marker antibodies with conjugated fluorophores. Zombie NIR is a fluorescent dye that cannot permeate live cells but can permeate dead cells because of their compromised membranes. CD4+ T cells were stained with 50 µl Zombie NIR (1:1000) per sample for 15 minutes at room temperature. During all incubation steps, samples were shielded from light. Subsequently, CD4+ T cells were washed with MACS buffer. Then, CD4+ T cells were stained with different fluorescent antibodies to assess the CD4+ T cell isolation and CD4+ T cell activation and Treg cells in the experiments. For that purpose, 50 µl of fluorescent antibody was added per sample and incubated for 20 minutes at room temperature. To assess the purity of the CD4+ T cell isolation, we analyzed three cell populations: cells collected from the lymph nodes and spleen before isolation, the positive fraction containing the CD4+ T cells after isolation, and the negative fraction containing all the remaining cells after isolation. These three populations were stained with Pacific Blue™ anti-mouse CD45.2 mAb (1:200), Brilliant Violet 570™ anti-mouse CD8a mAb (1:100), and APC anti-mouse CD4 mAb (1:250) (Table 1). CD4+ T cells from experiments were recovered for staining after culturing for 2 or 5 days. The CD4+ T cells were kept in or transferred to a U-bottom 96-well plate for staining and readout. For co-culture conditions, Falcon® 5 mL Round Bottom Polystyrene Test Tubes with Cell Strainer Snap Caps were used to filter out the organoids. CD4+ T cells were stained with APC anti-mouse CD4 mAb (1:250) and Pacific Blue™ anti-mouse CD25 mAb (1:250) (Table 1). After staining, the CD4+ T cells were washed with MACS buffer and, then, resuspended in 200 µl MACS buffer for analysis with the BD LSRFortessa™ Cell Analyzer. The obtained data were analyzed with FlowJo™ Software and Prism Graphpad 9.5.0 (Supplementary Figure 1).

Table 1 | Markers used for CD4+ T cell analysis using flow cytometry.

	Fluorophore	Dilution	Laser	Filter	Name	Company	Cat. No.
FOXP3	GFP		[488]	530_30-A			
CD4	APC	1:250	[640]	670_30-A	APC anti-mouse CD4 Antibody	BioLegend	100412
CD25	Pacific Blue	1:250	[405]	450_50-A	Pacific Blue™ anti-mouse CD25 Antibody	BioLegend	102022
CD8	BV570	1:100	[405]	610_20-A	Brilliant Violet 570™ anti-mouse CD8a Antibody	BioLegend	100739
CD45	Pacific Blue	1:200	[405]	450_50-A	Pacific Blue™ anti-mouse CD45.2 Antibody	BioLegend	109820
Zombie NIR		1:1000	[640]	780_60-A	Zombie NIR™ Fixable Viability Kit	BioLegend	423106

TGF-β concentration measured by ELISA

The Human TGF-β1 Quantikine™ ELISA kit was used to measure the TGF-β concentration in different conditioned media. Medium was collected from the bTL1 and dTSC1 organoid lines on day 3 of culturing. The medium and medium with matrix controls were also collected after 3 days of culturing. Medium from transwell co-cultures of bTL1 and dTSC1 organoid lines and Tact cells

were collected after 5 days of culturing. All media was stored at -80˚C. All standards, controls, and samples were assayed in duplicate. Controls and samples were activated according to the manufacturer's protocol. The optical density of each well was determined using a microplate reader set to 450 nm. The readouts of the duplicates from each standard, control, and sample were averaged. To calculate the concentration of the media of interest, a standard curve was created by plotting the mean absorbance for each standard against the concentration and fitting a linear trendline (Supplementary Figure 2).

Reagents

Product	Company	Cat. No.
Human TGF-β1 Quantikine™ ELISA kit	R&D systems	DB100B
T cell culture		
RPMI 1640 Medium, GlutaMAX™	Gibco	61870-010
FBS, heat-inactivated	Gemini Bio-Products	100-106
Penicillin–Streptomycin	Gibco	15140-122
Glutamax	Fisher Scientific	35050038
Sodium pyruvate	Gibco	11360-070
Nonessential amino acids	Gibco	11140-050
HEPES (N-2-hydroxyethylpiperazine-N-2-ethane sulfonic acid)	Gibco	15630-080
2-Mercaptoethanol	Sigma-Aldrich	M3148
Recombinant Human IL-2 Protein	PeproTech	200-02
Recombinant Human TGF-beta 1	R&D systems	7754-BH-025
CD3e Monoclonal Antibody (145-2C11), Functional Grade, eBioscience™	Invitrogen	16-0031-82
CD28 Monoclonal Antibody (37.51), Functional Grade, eBioscience	Invitrogen	16-0281-86
B6.Cg-Foxp3tm2Tch/J ("Foxp3EGFP" mice)	The Jackson Laboratory	JAX stock #006772
Organoid culture		
Advanced DMEM/F-12	Gibco	12634-010
Noggin conditioned medium	-	-
Recombinant Murine FGF-basic	PeproTech	450-33-50ug
N-Acetylcysteine	Sigma	A9165-5g
B-27™ Supplement (50X), serum free	Gibco	17504044
TrypLE™ Express Enzyme	Gibco	12604-021
Matrigel® Growth Factor Reduced (GFR) Basement Membrane Matrix, Phenol Red-free, *LDEV-free, 10 mL	Corning	356231, MG1: lot # 0337003; MG2: lot # 0090004
BME	R&D systems	lot # 1645405
GrowDex®	UPM	100103002
GrowDase™	UPM	900102001
Cell Recovery Solution	Corning	CLS354253
alamarBlue™ Cell Viability Reagent	Invitrogen	DAL1025
CD4+ T cell isolation		
CD4 (L3T4) MicroBeads, mouse	Miltenyi	130-117-043
LS Columns	Miltenyi	130-042-401

RESULTS

To study Treg cells in the TME of mesenchymal-CRC tumors, an *in vitro* co-culture system with murine CD4+ T cells and mesenchymal-CRC organoid lines was established. The extracellular matrix (ECM) in the TME plays an important role in the growth and development of the tumor *in vivo* (58). In cell culture, the ECM is mimicked by a matrix. Matrices are comprised of various components like fibrous proteins that form a molecular network to support the three-dimensional growth of organoids. Previous results in the lab showed that the matrix does not only have an effect on the growth of the organoid lines but also on CD4+ T cells when they are embedded in the matrix. To achieve our goal of cell-cell contact co-culture, it is crucial to assess the impact of different matrices on CD4+ T cells and mesenchymal-CRC organoid lines separately.

Among the different commercially available matrices are Cultrex Basement Membrane Extract (BME), Matrigel (MG), and GrowDex. We tested the effect of these three matrices on CD4+ T cells and mesenchymal-CRC organoid lines (bTL1 and dTSC1). BME and Matrigel are both produced using Engelbreth-Holm-Swarm (EHS) mouse sarcoma cells. These matrices are solubilized basement membrane extracts. The basement membrane is a thin layer of specialized extracellular matrix. Consequently, matrices consist of various ECM proteins like laminin and collagen. They also contain several growth factors that might have an undesirable effect on CD4+ T cells. In contrast, GrowDex is an animal-free hydrogel with natural nanofibers of cellulose extracted from wood. Because BME and Matrigel are animal products, they have a less defined composition regarding the ratio of their components than the animal-free GrowDex. The composition of BME and Matrigel can also differ more between batches. Therefore, two different batches of Matrigel were tested (MG1 and MG2). Taken together, these three matrices are different in composition and origin and therefore might differ in their effect on CD4+ T cells and mesenchymal-CRC organoid lines.

In every experiment, CD4+ T cells were analyzed using flow cytometry. We assessed the viability of the CD4+ T cells by determining the percentage of alive cells using Zombie NIR dye. Furthermore, we determined the activation status of CD4+ T cells by measuring the expression of the activation marker CD25 (CD4+CD25+ T cells) using the Median Fluorescent Intensity (MFI) of CD25. Lastly, we assessed the expression of the transcription factor FOXP3 as a marker to determine Treg cell percentage (CD4+CD25^{high}FOXP3gfp+ T cells).

Treg cell differentiation is induced in 50% matrix

With the final aim of establishing co-cultures with CD4+ T cells and mesenchymal-CRC organoid lines in matrix in mind, we first tested the effect of the different matrices on CD4+ T cells. As mentioned in the Materials and Methods section, the mesenchymal-CRC organoid lines are normally cultured in 50% BME. Thus, we tested the effect of 50% BME and Matrigel on CD4+ T cells. GrowDex needs to be used at a lower percentage of 0.25% because GrowDex has a different composition than BME and Matrigel. 50% BME and Matrigel and 0.25% GrowDex are plated as a droplet on the bottom of the well and medium is added on top (Figure 5A). Murine CD4+ T cells were plated in different conditions. Two control conditions were established where CD4+ T cells were plated in wells coated with anti-mouse CD3 monoclonal antibody (mAb) and cultured for five days; as a negative control, CD4+ T cells were activated (Tact cells) by adding 20 U/ml interleukin-2 (IL-2) and 1 µg/ml anti-mouse CD28 mAb to the medium and, for the positive control, Treg cells were induced (iTreg cells) by adding 300 U/ml IL-2, 1 µg/ml anti-mouse CD28 mAb, and 10 ng/ml TGF-β to the medium. The effect of the matrices on CD4+ T cells was first studied in the conventional medium for murine CD4+ T cells (enriched T cell medium, eTCM).

Later, the effect of the matrices was tested in murine organoid medium (BM2mouse, BM2m) because this medium is used in the co-culture assays.

Firstly, we checked the viability of the CD4+ T cells in the different matrices and observed that it is lower in 50% BME than in the other matrices (Figure 5B). Moreover, the activation of CD4+ T cells in all 50% matrices is lower compared to the Tact control condition in both media (Figure 5C, Supplementary Figure 3A). Moreover, we observed an increase in Treg cell percentage in 50% BME and Matrigel in BM2m medium and eTCM (Figure 5D, Supplementary Figure 3B). Treg cell induction is especially high in 50% BME with around 20% Treg cells in BM2m medium. This presents a challenge in our experimental plan for co-culture assays because the effect of the matrix could not be differentiated from the effect of mesenchymal-CRC organoid lines.

Treg cell induction is reduced in 10% matrix

To investigate if the induction of Treg cells by the matrix could be reduced by reducing the matrix percentage, CD4+ T cells were cultured in 10% matrix. 10% matrix is plated to fill the well instead of plating a droplet like with 50% matrix (Figure 5A). We observed an improvement in cell viability in 10% BME compared to 50% (Figure 5B). Furthermore, we found that the activation of the CD4+ T cells decreases similarly in BME and Matrigel compared to the Tact control condition in 10% matrix (Figure 5E). The CD4+ T cell activation is higher in 0.25% GrowDex than in 10% BME and Matrigel (Supplementary Figure 3C). Moreover, the results reveal that Treg cell induction is reduced in the conditions with 10% matrix compared to the ones with 50% matrix (Figure 5F, Supplementary Figure 3D). Lastly, there is no discernable difference between the two batches of Matrigel (Figure 5C-F, Supplementary Figure 3). In conclusion, Treg cell induction was reduced and the viability improved in 10% BME and Matrigel compared to 50% matrix. Therefore, 10% matrix is more suitable for CD4+ T cells to establish co-cultures with mesenchymal-CRC organoid lines because there is minimal effect from the matrix which allows analysis of the effect of the organoid lines.

Murine mesenchymal-CRC organoid lines grow in 10% BME and Matrigel

As previous experiments showed, 10% BME and Matrigel do not induce Treg cells. Therefore, a co-culture in 10% matrix would be the preferred condition to culture CD4+ T cells. Bearing in mind that the final aim was to establish co-cultures of CD4+ T cells and mesenchymal-CRC organoid lines, we aim to study the growth of the organoid lines in 10% matrices. The two organoid lines that were used, bTL1 and dTSC1, are commonly cultured in 50% matrix. Therefore, organoid line growth and viability were evaluated by imaging and an alamarBlue viability assay comparing 50 to 10% matrices and GrowDex (0.25 or 0.5%) (Figure 6A). Both organoid lines exhibited similar growth in terms of size and density in 10% matrices compared to 50% matrices when observed under a microscope (Figure 6B, C). However, both organoid lines grow at lower density in both percentages of GrowDex. Furthermore, the viability of the organoid lines in the different matrices was analyzed using an alamarBlue viability assay that measures the metabolic activity of the organoid lines (Figure 6D). The alamarBlue Cell Viability Reagent is a cell-permeable compound that is modified by the reducing environment of viable cells. The results from the viability assay confirmed the previous microscopy observation, organoid lines grow better in Matrigel and BME than in GrowDex. The viability of the bTL1 organoid line is slightly reduced in 10% matrices compared to 50% matrices (Figure 6E). However, upon re-examination of the imaging data of the bTL1 organoid line in 10% matrices we established that the organoid line growth is similar in 10 and 50% matrices. Therefore, we determined that 10% matrices are still suitable for culturing the bTL1 organoid line. Moreover, there is no difference in viability between the 10 and 50% matrix

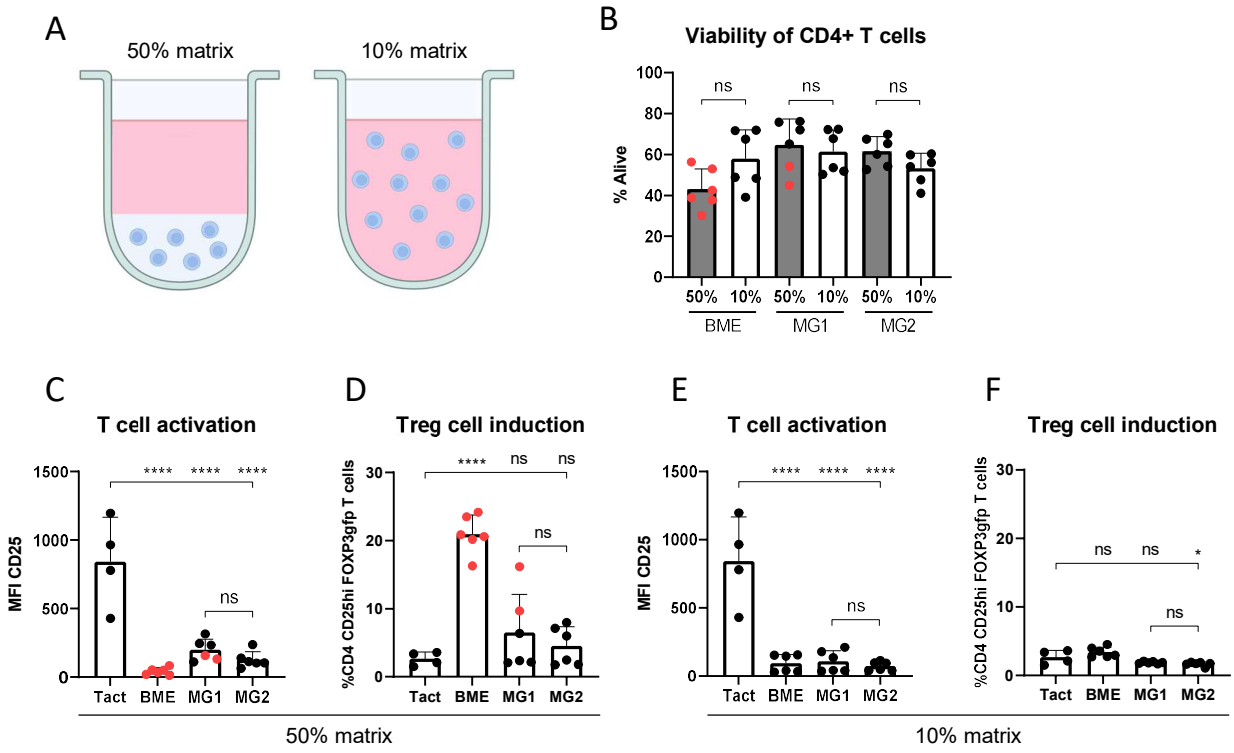

Figure 5 | Treg cells are induced by different matrices in BM2m medium. **(A)** Schematic representation of the culture of CD4+ T cells plated in 50 and 10% matrix. On day 5 of culture, the percentage of viable CD4+ T cells **(B)** plated in 10 or 50% BME or Matrigel was assessed using flow cytometry. **(C-F)** CD4+ T cell activation and the percentage of induced Treg cells upon culturing in 10 and 50% BME or Matrigel for 5 days were assessed using flow cytometry. CD4+ T cell activation is represented by the Median Fluorescent Intensity (MFI) of CD25. Data points with less than 3000 alive lymphocytes are represented as red circles. Data represented as means ± SD. (n=2). P-values were calculated using one-way ANOVA and unpaired t-test analysis. *p ≤ 0.05, **p ≤ 0.01, ***p ≤ 0.001, and ****p ≤ 0.0001, ns; not significant. Tact: activated CD4+ T cells.

with the dTSC1 organoid line, which is in line with previous observations (Figure 6F). Thus, the growth of bTL1 and dTSC1 organoid lines can be sustained in 10% BME and Matrigel.

Mesenchymal-CRC organoid lines induce Treg cells

To study the enrichment of Treg cells in CRC tumors (59), we established cell-cell contact co-cultures of CD4+ T cells with mesenchymal-CRC organoid lines (bTL1 and dTSC1) in 10% BME or Matrigel to study the effect of the organoid lines on the induction of Treg cells (Figure 7A-C). Previous experiments showed that 10% BME and Matrigel are the most suitable matrices to establish co-cultures with CD4+ T cells and mesenchymal-CRC organoid lines. The Tact control condition was used as a negative control and as an additional negative control, CD4+ T cells were activated in 10% matrices by adding 20 U/ml IL-2, 1 µg/ml anti-mouse CD3 mAb, and 1 µg/ml anti-mouse CD28 mAb to the matrix. In the co-culture conditions, CD4+ T cells are cultured together with the bTL1 or dTSC1 organoid line in 10% matrix and 20 U/ml IL-2, 1 µg/ml anti-mouse CD3 mAb, and 1 µg/ml anti-mouse CD28 mAb were added to activate CD4+ T cells. All conditions were cultured in BM2m medium. After 5 days of culturing, the percentage of Treg cells was determined using flow cytometry. The percentage of Treg cells increased upon co-culture of CD4+ T cells with bTL1 and dTSC1 organoid lines compared to the Tact condition in 10% BME (Figure 7D) and 10% Matrigel (Figure 7E). dTSC1 induced more Treg cells than bTL1 when

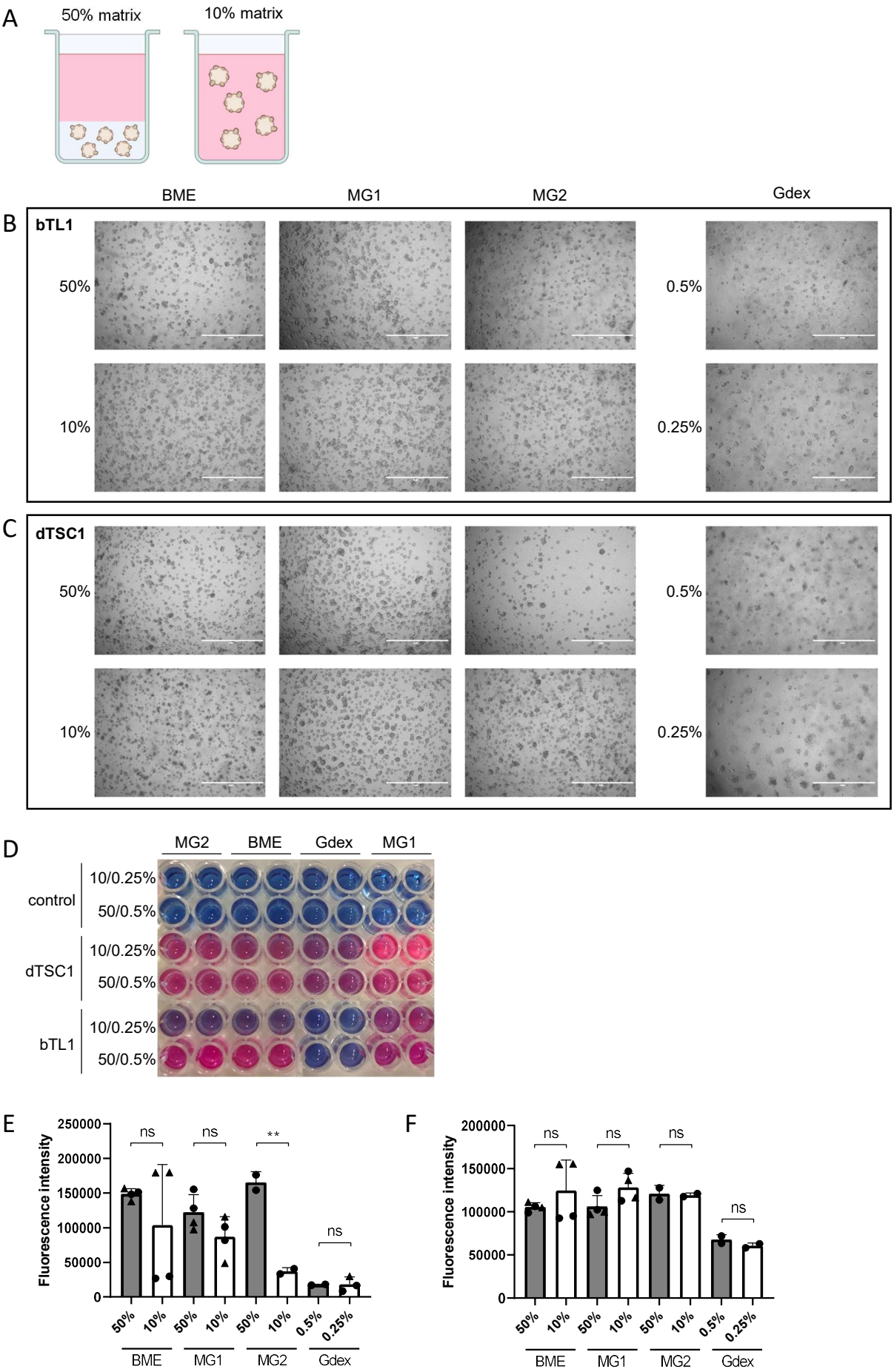

Figure 6 | bTL1 and dTSC1 organoid lines grow in 10% BME and Matrigel but less in GrowDex. Description continued on the next page.

Continued description from Figure 6. **(A)** Schematic representation of the culture of organoid lines in 50 and 10% matrix. Pictures of **(B)** bTL1 and **(C)** dTSC1 organoid lines in different matrices on day 4 of culture captured on an EVOS brightfield microscope at 4x magnification. The scale bars represent 1000 µm. **(D)** Plate layout of the alamarBlue assay with controls (medium and matrix), bTL1, and dTSC1 organoid lines in different matrices. The viability of **(E)** bTL1 and **(F)** dTSC1 organoid lines cultured in different matrices was assessed with an alamarBlue assay on day 4 of culture. The circles and the triangles represent technical duplicates of two independent experimentsData represented as means ± SD. P-values were calculated using one-way ANOVA and unpaired t-test analysis. *p ≤ 0.05, **p ≤ 0.01, ***p ≤ 0.001, and ****p ≤ 0.0001, ns; not significant.

co-cultured with CD4+ T cells independently of the used matrix, BME (Figure 7F) or Matrigel (Figure 7G). The induction of Treg cells by both organoid lines was slightly higher in the conditions plated in BME as matrix. In conclusion, bTL1 and dTSC1 organoid lines induce Treg cells upon co-culture with CD4+ T cells in 10% BME and Matrigel.

The induction of Treg cells by mesenchymal-CRC organoid lines is TGF-β dependent

TGF-β has a crucial role in the differentiation and function of Treg cells (9). Through its signaling pathway, TGF-β induces expression of the transcription factor FOXP3, which is essential for Treg cell differentiation and function. TGF-β is available in the TME of mesenchymal-CRC tumors. Therefore, we studied whether the observed Treg cell induction by the mesenchymal-CRC organoid lines is TGF-β dependent. To this end, a TGF-β receptor I kinase inhibitor (SB-431542, SB) was added to the medium of the co-culture and control conditions. We observed that induction of Treg cells by the organoid lines was significantly reduced by the addition of SB (Figure 7F, G). These results confirmed that the induction of Treg cells by mesenchymal-CRC organoid lines is TGF-β dependent. To confirm that the organoid lines secrete TGF-β, TGF-β concentration was determined in the medium from the organoid lines cultured with or without CD4+ T cells by ELISA (Figure 7H). The medium from organoid lines was collected after 3 days of culturing and the medium from co-cultures after 5 days of culturing. The results from the ELISA showed that CD4+ T cells and BME matrix alone do not increase TGF-β concentration in the medium compared to the control with only medium. Furthermore, TGF-β concentration is slightly, but not significantly, elevated in the medium of both organoid lines compared to the control with medium and BME. There is no difference between the TGF-β concentration in the medium of bTL1 and dTSC1 organoid lines. However, TGF-β concentration significantly increased in the medium of the co-cultures with both bTL1 and dTSC1 organoid lines compared to the control with medium and BME. In the co-culture medium of dTSC1 organoid line with CD4+ T cells TGF-β concentration is higher than in the co-culture medium of bTL1 organoid line with CD4+ T cells. In conclusion, bTL1 and dTSC1 organoid lines induce Treg cells in a TGF-β-dependent manner upon co-culture with CD4+ T cells in 10% BME and Matrigel. Furthermore, Treg cell induction and TGF-β concentration in the medium are higher in co-cultures with the dTSC1 organoid line than with the bTL1 organoid line.

Lactate does not affect CD4+ T cell activation and Treg cell induction in eTCM

To further study Treg cell differentiation in the TME, a system without organoid lines was established. Previous experiments showed the essential role of TGF-β in the induction of Treg cells by mesenchymal-CRC organoid lines. Besides TGF-β, the high lactate concentration in the TME plays an important role in the enrichment of Treg cells. Treg cells, unlike other immune cells, can

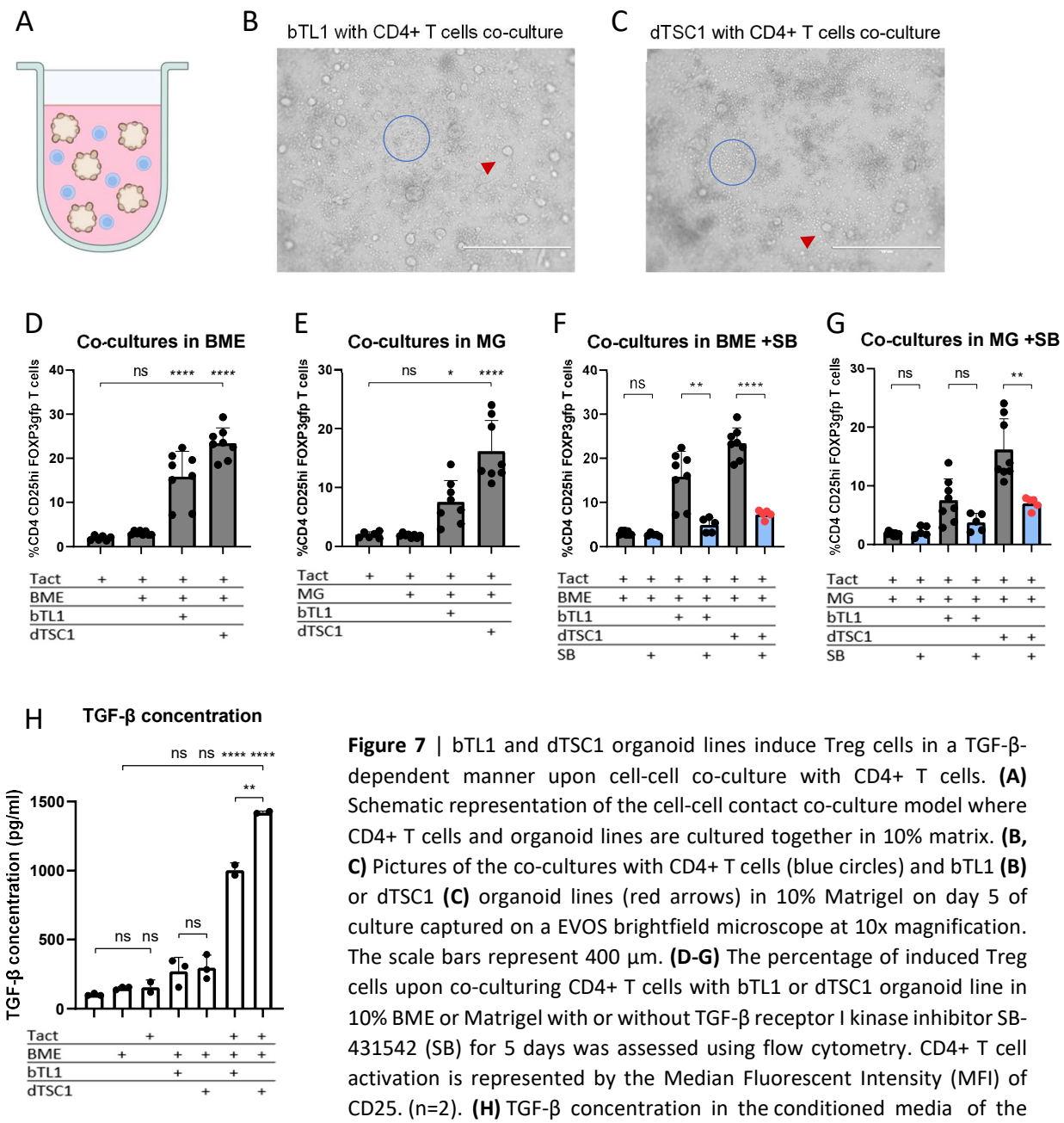

Figure 7 | bTL1 and dTSC1 organoid lines induce Treg cells in a TGF-β-dependent manner upon cell-cell co-culture with CD4+ T cells. **(A)** Schematic representation of the cell-cell contact co-culture model where CD4+ T cells and organoid lines are cultured together in 10% matrix. **(B, C)** Pictures of the co-cultures with CD4+ T cells (blue circles) and bTL1 **(B)** or dTSC1 **(C)** organoid lines (red arrows) in 10% Matrigel on day 5 of culture captured on a EVOS brightfield microscope at 10x magnification. The scale bars represent 400 µm. **(D-G)** The percentage of induced Treg cells upon co-culturing CD4+ T cells with bTL1 or dTSC1 organoid line in 10% BME or Matrigel with or without TGF-β receptor I kinase inhibitor SB-431542 (SB) for 5 days was assessed using flow cytometry. CD4+ T cell activation is represented by the Median Fluorescent Intensity (MFI) of CD25. (n=2). **(H)** TGF-β concentration in the conditioned media of the bTL1 and dTSC1 organoid lines alone and of their co-cultures with CD4+ T cells was measured by ELISA. Medium from conditions with no supplements, with matrix, and with Tact cells were used as negative controls. Data points with less than 3000 alive lymphocytes are represented as red circles. Data represented as means ± SD. P-values were calculated using one-way ANOVA and unpaired t-test analysis. *p ≤ 0.05, **p ≤ 0.01, ***p ≤ 0.001, and ****p ≤ 0.0001, ns; not significant. Tact: activated CD4+ T cells.

change their metabolism to survive in high lactate concentrations (47). The switch to lactate metabolism also increases the immunosuppressive function of Treg cells. Therefore, we wanted to study the combined effect of TGF-β and lactate on CD4+ T cells. To test the effect of TGF-β and lactate on CD4+ T cells, we supplemented them to the medium of CD4+ T cells in culture. Here, the Tact condition is used as a negative control and the iTreg condition is used as a positive control. CD4+ T cells were cultured in eTCM or BM2m medium with different TGF-β concentrations with or without lactate. After 5 days of culturing, CD4+ T cells were collected and analyzed by flow cytometry to assess the percentage of Treg cells and CD4+ T cell activation.

Firstly, the effect of TGF-β and lactate on CD4+ T cell activation and Treg cell induction was studied in eTCM. The induction of Treg cells was similar in all TGF-β concentrations (Figure 8A). Furthermore, lactate had no effect on Treg cell induction with low (1 ng/ml) or high (10 ng/ml) TGF-β concentration (Figure 8B, C). In addition, a different approach for the induction of Treg cells in eTCM was tried in which anti-mouse CD3 mAb is added in suspension in the medium rather than coated on the plate. Here, the percentage of Treg cells was decreased to 10% whereas it was 40% with the coated anti-mouse CD3 mAb after culturing for five days (Figure 8D). However, the percentage of Treg cells is higher on day 2 than on day 5 with the anti-mouse CD3 mAb in suspension (Supplementary Figure 4). These observations are contrary to the results with coated anti-mouse CD3 mAb where the percentage of Treg cells increases over time. Although the percentage of Treg cells was lower in conditions with anti-mouse CD3 mAb in suspension, the Treg cell induction was similar in all TGF-β concentrations. Furthermore, the addition of lactate did not affect the induction of Treg cells in either low or high TGF-β concentration regardless of the condition of anti-mouse CD3 mAb (Figure 8E, F). Overall, Treg cell induction is optimal at day 5 with anti-mouse CD3 mAb coated on the plate instead of in suspension in the medium. The lower percentage of Treg cells on day 5 with anti-mouse CD3 mAb in suspension could be explained by the exhaustion of the CD4+ T cells on day 5. Moreover, there was no difference in Treg cell induction between low and high TGF-β concentrations or with or without lactate added to eTCM.

Increasing TGF-β concentration increases Treg cell induction in eTCM without pyruvate

Pyruvate is one of the components of eTCM. Lactate and pyruvate are closely related in cellular metabolism because lactate can be converted into pyruvate and vice versa by lactate dehydrogenase (LDH) (60). Pyruvate can be transported to the mitochondria where it is used in the TCA cycle for energy production. Hence, pyruvate in eTCM might be masking the effect of lactate on Treg cell differentiation. Therefore, previous experiments with CD4+ T cells in increasing TGF-β concentrations with or without lactate were repeated with eTCM without pyruvate. In addition, TGF-β concentration was further decreased to 0.1 ng/ml because there was no discernable difference between the induction of Treg cell differentiation at 1 or 10 ng/ml TGF-β. We observed an increase in the percentage of Treg cells with increasing TGF-β concentration (Figure 8G). These results differ from the results in eTCM with pyruvate where there was no difference in Treg cell induction between 1 and 10 ng/ml TGF-β concentration. Besides that, lactate does not affect the induction of Treg cell differentiation irrespective of the TGF-β concentration (Figure 8H, I). Thus, pyruvate in the eTCM was not masking the effect of lactate on Treg cell differentiation.

Lactate induces CD4+ T cell activation in BM2m medium

Considering that the induction of Treg cell differentiation by the mesenchymal-CRC organoid lines is in the context of BM2m medium, this medium was also assessed for the induction of Treg cells with different TGF-β concentrations with or without lactate. We observed an increase in the induction of Treg cell differentiation with increasing TGF-β concentration like in eTCM without pyruvate (Figure 8J). However, no effect on Treg cell differentiation is observed by supplementing BM2m medium with lactate (Figure 8K, L). Furthermore, CD4+ T cell activation was lower in the conditions with TGF-β compared to the Tact control (Supplementary Figure 5A). Lactate increased CD4+ T cell activation in low (0.1 ng/ml) and high (10 ng/ml) TGF-β concentrations conditions (Supplementary Figure 5B, C). However, this increase in CD4+ T cell activation is not an increase in the percentage of CD4+CD25+ T cells (Supplementary Figure 5D, E) but an increase

in CD25 expression by the activated CD4+ T cells measured by the MFI of CD25. We compared the CD25 expression of CD25+FOXP3- and CD25+FOXP3+ T cells (Supplementary Figure 5F, G) and found that the CD25 expression increases as a result of lactate in both populations. In conclusion, lactate does not induce Treg cells but does increase the activation in the general CD4+CD25+ T cell population.

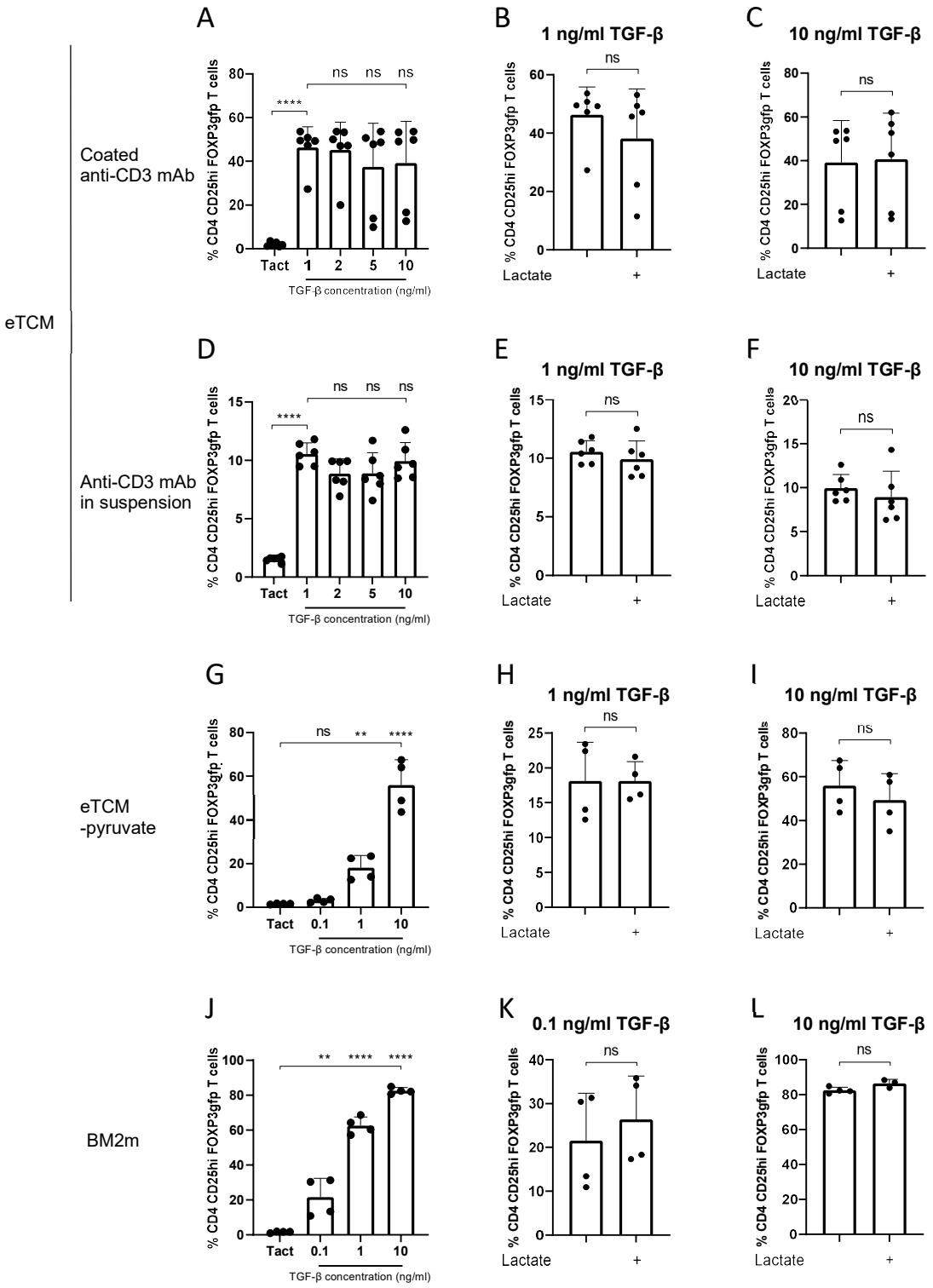

Figure 8 | TGF-β increases Treg cell induction but lactate does not affect Treg cell induction. CD4+ T cells were analyzed on day 5 using flow cytometry. The effect of TGF-β and lactate on Treg cells was studied in eTCM with coated anti-mouse CD3 mAb **(A-C)**, eTCM with anti-mouse CD3 mAb in suspension **(D-F)**, eTCM without pyruvate **(G-I)**, and BM2m medium **(J-L)**. The first graph for each medium represents the percentage of Treg cells in Tact condition (negative control) and in conditions with increasing TGF-β concentration. The second and third graphs for each medium represent the percentage of Treg cells in low and high TGF-β concentrations with or without lactate. Data represented as means ± SD. (n=3 for conditions in eTCM; n=2 for conditions in eTCM without pyruvate and in BM2m medium). P-values were calculated using one-way ANOVA and unpaired t-test analysis. *p ≤ 0.05, **p ≤ 0.01, ***p ≤ 0.001, and ****p ≤ 0.0001, ns; not significant. Tact: activated CD4+ T cells.

DISCUSSION

In this study, we explore the mechanisms involved in the induction of Treg cells from CD4+ T cells upon co-culture with mesenchymal-CRC organoid lines (bTL1 and dTSC1). For this purpose, we developed an *in vitro* system of cell-cell contact co-cultures with murine CD4+ T cells and mesenchymal-CRC organoid lines. While in human CD4+ T cells, *FOXP3* is also transiently expressed in a subset of activated CD4+ T cells that are non-regulatory, in mice only Treg cells express *FOXP3* (61–63). Therefore, *FOXP3* expression is sufficient to identify Treg cells among murine CD4+ T cells. To study the effect of mesenchymal-CRC organoid lines on Treg cells, we used the transgenic Foxp3EGFP mice in which Treg cells express GFP by having *FOXP3* and GFP under the endogenous *FOXP3* promoter. This model allows us to analyze the Treg cell population upon co-culture of CD4+ T cells with mesenchymal-CRC organoid lines by flow cytometry.

Previous results in the lab have shown that the matrix (BME and Matrigel) at 50% used for organoid culture affects CD4+ T cells, hampering reliable analysis of the Treg cell population upon co-culture with mesenchymal-CRC organoid lines. Therefore, we tested the effect of different matrices (BME and Matrigel) generally used for organoid culture on CD4+ T cells before establishing co-cultures with the mesenchymal-CRC organoid lines. We found that Treg cell induction is higher upon culturing CD4+ T cells embedded in 50% BME than in 50% Matrigel. We hypothesize that the undesired Treg cell induction in 50% BME could be due to properties of the used extracellular matrix. As BME and Matrigel are derived from mouse sarcoma cells, they are known to contain several growth factors. One of the factors present in the matrices could be TGF-β, which was shown in our experiments to be crucial for Treg cell induction. Therefore, we decreased the percentage of matrix used for culturing CD4+ T cells from 50 to 10%, expecting to reduce Treg cell induction. Here, we saw no induction of Treg cells from CD4+ T cells in either of the tested matrices. Furthermore, the activation of CD4+ T cells was lower in both matrices compared to the pTact condition. This lower activation could be an effect of reduced diffusion of the anti-mouse CD3 and anti-mouse CD28 mAbs used to activate CD4+ T cells. Taken together, the experiments with CD4+ T cells in different matrices revealed that 10% BME and Matrigel are the most suitable for culturing CD4+ T cells in a matrix. Highlighting this, we cannot ignore the effect that the matrix can have on CD4+ T cells when cultured embedded in the matrix. This finding is especially important because experiments with cells in matrix are regularly performed in various fields of study, potentially without paying enough attention to the effect of the matrix.

In addition and because the final aim was to establish co-cultures with CD4+ T cells and mesenchymal-CRC organoid lines (bTL1 and dTSC1), we tested the effect of the different matrices on the organoid lines. Mesenchymal-CRC organoid lines are usually cultured in 50% BME to support their growth in a 3D structure. Here, we tested the organoid growth in 10% BME or Matrigel and 0.25 or 0.5% GrowDex. We used imaging and an alamarBlue viability assay to evaluate the viability of the mesenchymal-CRC organoid lines in different matrices. Although the alamarBlue assay determined the growth of the mesenchymal-CRC organoid lines in the different matrices, there are concerns about the assay's reliability when it comes to determining organoid viability. The alamarBlue assay is developed to measure viability in single-cell suspensions but is also used in matrix-containing cultures (64). However, the more common method to determine organoid viability is with a CellTiter-Glo Luminescent Cell Viability Assay as used by Xie and Wu in order to determine the viability of patient-derived CRC organoids (65). The CellTiter-Glo Reagent lyses cells and is modified by the presence of ATP. To potentially get a more reliable measurement of organoid viability, a viability assay with CellTiter-Glo instead of alamarBlue could be performed. However, from our microscopy observations and the alamarBlue assay, we can conclude that the growth of both mesenchymal-CRC organoid lines is hampered in GrowDex.

Conversely, we found that the growth of these mesenchymal-CRC organoid lines is supported in 10% BME and Matrigel.

Considering the promising results of experiments with CD4+ T cells and mesenchymal-CRC organoid lines in 10% matrix separately, we proceeded to establish a cell-cell contact co-culture system with CD4+ T cells and mesenchymal-CRC organoid lines in 10% BME and Matrigel. We showed that mesenchymal-CRC organoid lines induce Treg cells upon 5 days of co-culture. Previous studies showed the importance of TGF-β signaling in Treg cell differentiation and function (9). Therefore, we hypothesized that the mesenchymal-CRC organoid lines induced Treg cells in a TGF-β-dependent manner and evaluated the influence of TGF-β in the co-cultures. For that purpose, we added a TGF-β receptor I kinase inhibitor (SB-431542) to the co-cultures. Here, we observed a diminished Treg cell induction, demonstrating the critical role of TGF-β in this system. As explained before, a high population of Treg cells in the TME of mesenchymal-CRC has been associated with a poor prognosis (43). Therefore, a reduction in Treg cells by the TGF-β receptor I kinase inhibitor could be relevant for CRC therapy. TGF-β receptor I kinase inhibitors are already studied in clinical trials for various cancers such as glioblastoma, hepatocellular carcinoma, and pancreatic cancer where some anti-tumor effects were observed (66). These experiments showed that TGF-β receptor I kinase inhibitor could also potentially be relevant for CRC treatment because it prevents Treg cell induction by mesenchymal-CRC organoid lines.

In parallel, we studied whether TGF-β is secreted into the medium of co-cultures with mesenchymal-CRC organoid lines and CD4+ T cells by performing an ELISA. We observed an increase in TGF-β concentration in the medium of co-cultures compared to CD4+ T cells or mesenchymal-CRC organoid lines alone. These results are in line with previous results that showed that Treg cell induction by mesenchymal-CRC organoid lines is TGF-β dependent. However, medium from the mesenchymal-CRC organoid lines was collected on day 3 of culturing while the medium from transwell co-cultures was collected after 5 days of culturing. It could be that the organoid lines alone also secrete TGF-β after 5 days of culture when they are more developed. Therefore, this ELISA should be repeated with all media collected on day 5. Furthermore, we observed a correlation between higher TGF-β concentration and Treg induction in co-cultures with the dTSC1 organoid line compared to lower TGF-β concentration and Treg induction with the bTL1 organoid line. However, we need to investigate whether the mesenchymal-CRC organoid lines, CD4+ T cells, or both secrete TGF-β in this setup. We could investigate whether the mesenchymal-CRC organoid lines secrete TGF-β with a co-culture with TGF-β knockout mesenchymal-CRC organoid lines. If the mesenchymal-CRC organoid lines secrete TGF-β, TGF-β secretion should be inhibited in the setup with TGF-β knockout mesenchymal-CRC organoid lines. In that case, TGF-β concentration in the medium would be reduced. Alternatively, we could measure the expression of TGF-β in mesenchymal-CRC organoid lines and CD4+ T cells alone compared to expression in co-culture using RT-PCR. Moreover, we want to investigate the importance of other potential secreted factors in the medium involved in Treg cell induction in the co-cultures with mesenchymal-CRC organoids and CD4+ T cells. We could discover potential other secreted factors in the medium with proteomics. Previous results from the lab showed that conditioned medium from the mesenchymal-CRC organoid lines does not induce Treg cells. The lack of Treg cell induction by the conditioned medium from the mesenchymal-CRC organoid lines correlates with our observation that the organoid lines alone do not secrete TGF-β into the medium. It would be interesting to culture CD4+ T cells with conditioned medium from co-cultures because we observed that more TGF-β is secreted in the co-culture conditions than with the mesenchymal-CRC organoid lines alone. We expect the TGF-β containing medium from co-cultures with mesenchymal-CRC organoid lines and CD4+ T cells to induce Treg cells. Furthermore, we need to investigate whether the observed Treg cell induction is due to TGF-β-driven conversion of CD4+ T cells to Treg cells or survival and proliferation of Treg cells. We can

study this using co-cultures with mesenchymal-CRC organoid lines and FOXP3-sorted CD4+ T cells. In this experiment, CD4+ T cells would be sorted into three populations using FACS: FOXP3 positive and negative, FOXP3 positive, and FOXP negative CD4+ T cells. The FOXP3-sorted CD4+ T cells would be stained with CellTrace™ Violet (CTV) to be able to follow their proliferation. Then, we would establish co-cultures with these three populations of CD4+ T cells and mesenchymal-CRC organoid lines. By analyzing the proliferation in each of the three CD4+ T cell populations using flow cytometry, we could determine whether conversion, survival, or proliferation of Treg cells plays a role in the observed Treg cell induction upon co-culture of CD4+ T cells with mesenchymal-CRC organoid lines.

Moreover, an *in* vitro suppression assay could be used to verify the immunosuppressive function of the Treg cells induced by the mesenchymal-CRC organoid lines (67). In a suppression assay, CD4+ T cells are separated from the organoids using a filter that only lets CD4+ T cells through and not organoids. Then, CD4+ T cells from the co-culture are cultured together with CTV-stained Teff cells. After 3-5 days, the proliferation of the Teff cells is measured using the CTV staining in flow cytometry. If the Treg cells among the CD4+ T cells are immunosuppressive, the proliferation of the Teff cells is reduced.

Additionally, we investigated the combined effect of lactate and TGF-β in the induction of Treg cells from CD4+ T cells because of their important role in Treg cell enrichment in the TME of mesenchymal-CRC tumors (9,43,45,46). Treg cells exhibit metabolic flexibility, enabling them to use lactate as a source of energy whereas other immune cells such as Teff cells cannot survive in a high lactate environment because they cannot use lactate as an energy source (47). Therefore, we expected higher induction of Treg cells by supplementing lactate to the medium of CD4+ T cells in culture. To study the role of lactate under different concentrations of TGF-β, we cultured CD4+ T cells in medium with increasing concentrations of TGF-β with or without lactate and the Tact condition as a negative control. We first cultured CD4+ T cells in eTCM because this is the conventional medium for culturing murine CD4+ T cells. Here, we found no difference in Treg cell induction between different TGF-β concentrations. Furthermore, we did not observe an effect of lactate on Treg cell induction in low or high concentrations of TGF-β. We hypothesize that this could be an effect of the FBS in the medium. FBS is a widely used growth supplement in cell culture that contains several proteins, nutrients, and growth factors that might promote Treg cells. Therefore, it would be interesting to repeat the experiments with increasing TGF-β concentration in a medium without FBS. The FBS in eTCM could be substituted with serum-free B-27 cell culture supplement (68). Furthermore, pyruvate is a component of eTCM and it is closely related to lactate in cellular metabolism because lactate is converted into pyruvate. Pyruvate is transported to the mitochondria and used in the TCA cycle. Hence, we hypothesized that pyruvate could be masking the effect of lactate on Treg cell induction in eTCM. Therefore, we repeated the experiments with different TGF-β concentrations with or without lactate in eTCM without pyruvate. Here, induction of Treg cells increases with increasing TGF-β concentrations. However, we did not observe an effect of lactate on Treg cell induction in low or high concentrations of TGF-β. The results of our experiments with supplemented TGF-β confirmed the positive effect of TGF-β on the induction of Treg cells *in vitro*. To further investigate this correlation *in vivo*, immunohistochemistry stainings could be done for Treg cells and TGF-β in murine CRC tumors. We hypothesize that Treg cells would be more enriched in tumors with a higher TGF-β concentration. To investigate this, anti-FOXP3 and anti-TGF-β antibodies would be used on CRC tumors isolated from mice (69,70). Then, we would analyze the correlation between TGF-β concentration and Treg cell presence.

Lastly, we repeated the experiments with increasing TGF-β concentrations with or without lactate in BM2mouse medium because this is the medium used for co-cultures. Here, we observed an increase in Treg cell induction with increasing TGF-β concentrations. We also analyzed the CD4+ T cell activation using the percentage of CD4+CD25+ T cells and the MFI of CD25. In this way,

we do not only determine the percentage of activated CD4+ T cells but also the expression level of CD25. We found that lactate induces an increase in CD25 expression by CD4+ T cells but not in Treg cell induction with low and high concentrations of TGF-β. Interestingly, we do not observe an increase in the percentage of CD4+CD25+ T cells. This implies that the population of activated CD4+ T cells does not increase but the expression of CD25 by the activated CD4+ T cells does. We expected higher expression of CD25 in Treg cells in conditions supplemented with lactate. To study this, we analyzed which population of CD4+ T cells exhibited increased CD25 expression by comparing the effect of lactate on CD4+ T cell activation in the CD25+FOXP3- and CD25+FOXP3+ T cell populations. We found that there is higher activation in both cell populations and not just in Treg cells. Further research is required to fully understand how lactate affects CD4+ T cell activation in FOXP3+ and FOXP3- T cells in the presence of TGF-β.

The analysis for several experiments in this study was done with only two independent experiments (n=2). We understand that this reduces the reliability of the results and that the experiments need to be repeated to reach n=3. In addition, there were less than 3000 alive lymphocytes in various conditions in the experiments analyzed with flow cytometry. In the analysis of flow cytometry data, we aim for 10,000 alive lymphocytes to get a reliable analysis (Supplementary Figure 1). Thus, the analysis of conditions with less than 3000 alive lymphocytes is less reliable.

This study revealed that mesenchymal-CRC organoid lines induce Treg cells in a TGF-β-dependent manner upon cell-cell contact co-culture with CD4+ T cells. The increase of Treg cell induction with increasing TGF-β concentrations was shown in CD4+ T cell culture and in co-cultures of CD4+ T cells with mesenchymal-CRC organoid lines. Furthermore, the Treg cell induction by the mesenchymal-CRC organoid lines was reduced when a TGF-β receptor I kinase inhibitor was added. Treg cells are an interesting therapeutical target because a high number of Treg cells in the tumor is indicative of a poor prognosis. The co-culture model with CD4+ T cells and mesenchymal-CRC organoid lines will help the field to better understand Treg cells in the TME of mesenchymal-CRC tumors. The TME is an interesting target for therapy because it is crucial for tumor progression and growth. Different treatment strategies targeting the TME already exist or are being explored (71). It is important to gain a better understanding of how we can target the immunosuppressive TME of mesenchymal-CRC tumors because of the lack of effective therapies against mesenchymal-CRC tumors.

SUPPLEMENTARY FIGURES

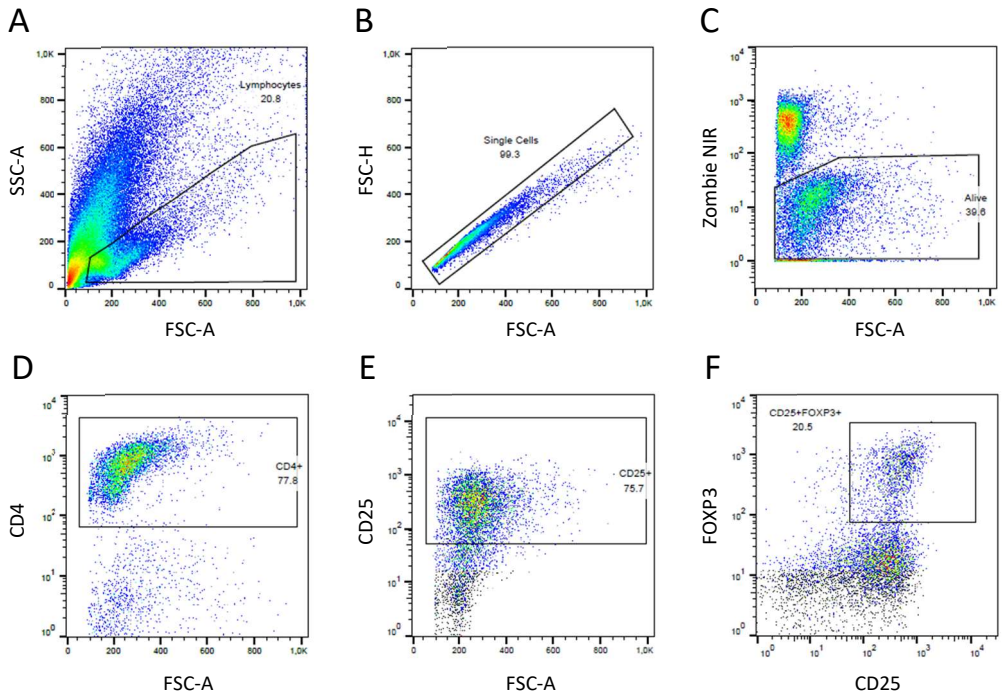

Supplementary figure 1 | Gating strategy used to analyze the CD4+ T cells with FlowJo™ Software. **(A)** Lymphocytes selected from all recorded events. **(B)** Single cells selected from lymphocytes. **(C)** Alive cells (Zombie NIR negative) selected from single cells. **(D)** CD4+ T cells selected from alive cells. **(E)** CD25+ T cells selected from CD4+ T cells. **(F)** CD25+FOXP3+ T cells selected from CD4+ T cells.

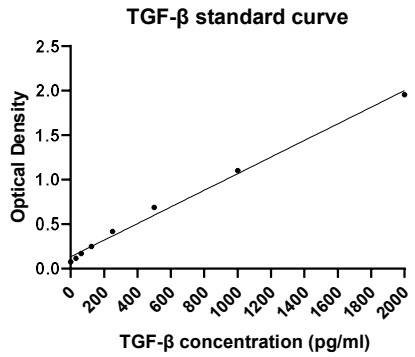

Supplementary figure 2 | TGF-β concentration ELISA standard curve.

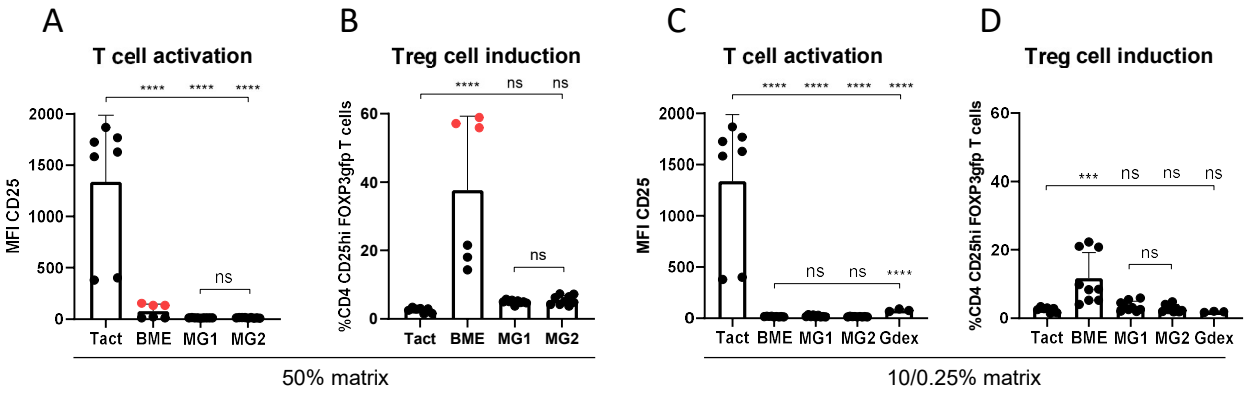

Supplementary figure 3 | Treg cells can be induced by different matrices in eTCM. **(A-D)** CD4+ T cell activation and the percentage of induced Treg cells upon culturing in 10 and 50% BME or Matrigel and 0.25 and 0.5% GrowDex for 5 days were assessed using flow cytometry. CD4+ T cell activation is represented by the Median Fluorescent Intensity (MFI) of CD25. Data points with less than 3000 alive lymphocytes are represented as red circles. Data represented as means ± SD. (n=3). P-values were calculated using one-way ANOVA and unpaired t-test analysis. *p ≤ 0.05, **p ≤ 0.01, ***p ≤ 0.001, and ****p ≤ 0.0001, ns; not significant. Tact: activated CD4+ T cells.

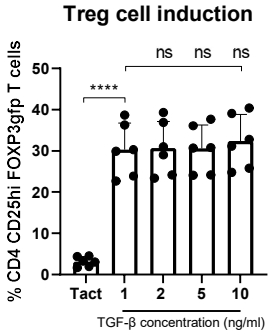

Supplementary figure 4 | Treg cells are induced in eTCM with anti-CD3 Ab in suspension on day 2. CD4+ T cells were analyzed using flow cytometry. The graph represents the percentage of Treg cells in Tact condition (negative control) and in conditions with 1, 2, 5, or 10 ng/ml TGF-β supplemented to eTCM with anti-mouse CD3 Ab in suspension. Data represented as means ± SD. (n=3). P-values were calculated using one-way ANOVA and unpaired t-test analysis. *p ≤ 0.05, **p ≤ 0.01, ***p ≤ 0.001, and ****p ≤ 0.0001, ns; not significant. Tact: activated CD4+ T cells.

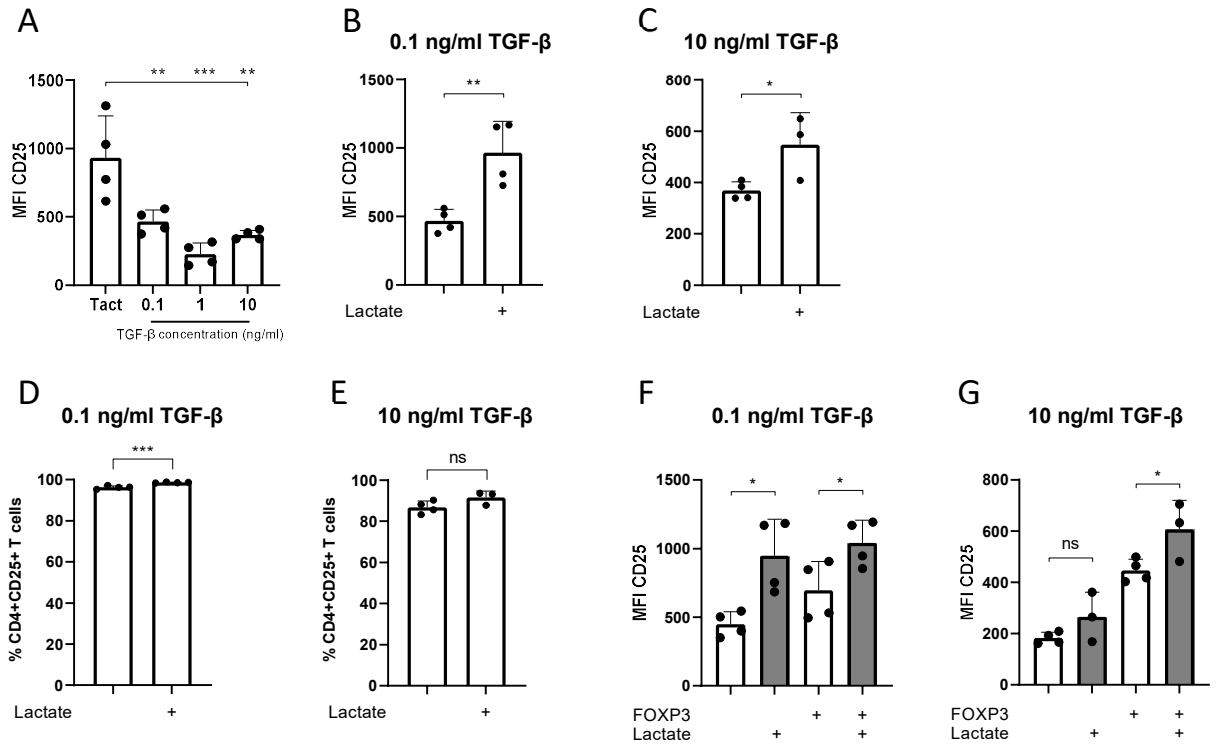

Supplementary Figure 5 | Lactate increases CD4+ T cell activation with different TGF-β concentrations in BM2m medium. **(A)** CD4+ T cell activation in Tact condition (negative control) and in conditions with increasing TGF-β concentration. CD4+ T cell activation is represented by the Median Fluorescent Intensity (MFI) of CD25. **(B, C)** CD4+ T cell activation in low **(B)** and high **(C)** TGF-β concentration with or without lactate. **(D, E)** Percentage of activated CD4+ T cells in low **(D)** and high **(E)** TGF-β concentration with or without lactate. **(F, G)** CD4+ T cell activation in the CD25+FOXP3- and CD25+FOXP3+ T cell population with low **(F)** and high **(G)** TGF-β concentration with or without lactate. Data represented as means ± SD. (n=2). P-values were calculated using one-way ANOVA and unpaired t-test analysis. *p ≤ 0.05, **p ≤ 0.01, ***p ≤ 0.001, and ****p ≤ 0.0001, ns; not significant. Tact: activated CD4+ T cells.

LITERATURE

1. Sakaguchi S, Yamaguchi T, Nomura T, Ono M. Regulatory T cells and immune tolerance. Cell. 2008 May 30;133(5):775–87.

2. Gershon RK, Kondo K. Cell interactions in the induction of tolerance: the role of thymic lymphocytes. Immunology. 1970 May;18(5):723–37.

3. Fontenot JD, Gavin MA, Rudensky AY. Foxp3 programs the development and function of CD4+CD25+ regulatory T cells. Nat Immunol. 2003 Apr;4(4):330–6.

4. Hori S, Nomura T, Sakaguchi S. Control of regulatory T cell development by the transcription factor Foxp3. Science. 2003 Feb 14;299(5609):1057–61.

5. Dembic Z, Beginning of the end of (understanding) the immune response. Scand J Immunol. 2008 Oct;68(4).

6. Zhang X, Izikson L, Liu L, Weiner HL. Activation of CD25(+)CD4(+) regulatory T cells by oral antigen administration. J Immunol Baltim Md 1950. 2001 Oct 15;167(8).

7. Aluvihare VR, Kallikourdis M, Betz AG. Regulatory T cells mediate maternal tolerance to the fetus. Nat Immunol. 2004 Mar;5(3).

8. Shevyrev D, Tereshchenko V. Treg Heterogeneity, Function, and Homeostasis. Front Immunol. 2019;10:3100.

9. Chen W, Jin W, Hardegen N, Lei KJ, Li L, Marinos N, et al. Conversion of peripheral CD4+CD25- naive T cells to CD4+CD25+ regulatory T cells by TGF-beta induction of transcription factor Foxp3. J Exp Med. 2003 Dec 15;198(12):1875–86.

10. Zheng SG, Wang J, Wang P, Gray JD, Horwitz DA. IL-2 is essential for TGF-beta to convert naive CD4+CD25- cells to CD25+Foxp3+ regulatory T cells and for expansion of these cells. J Immunol Baltim Md 1950. 2007 Feb 15;178(4):2018–27.

11. Hsieh CS, Zheng Y, Liang Y, Fontenot JD, Rudensky AY. An intersection between the self-reactive regulatory and nonregulatory T cell receptor repertoires. Nat Immunol. 2006 Apr;7(4):401–10.

12. Nguyen DD, Snapper SB. Targeting Smads to Restore Transforming Growth Factor-β Signaling and Regulatory T-Cell Function in Inflammatory Bowel Disease. Gastroenterology. 2009 Apr 1;136(4):1161–4.

13. Zheng Y, Josefowicz S, Chaudhry A, Peng XP, Forbush K, Rudensky AY. Role of conserved non-coding DNA elements in the Foxp3 gene in regulatory T-cell fate. Nature. 2010 Feb 11;463(7282):808–12.

14. Okeke EB, Uzonna JE. The Pivotal Role of Regulatory T Cells in the Regulation of Innate Immune Cells. Front Immunol. 2019;10:680.

15. Brunkow ME, Jeffery EW, Hjerrild KA, Paeper B, Clark LB, Yasayko SA, et al. Disruption of a new forkhead/winged-helix protein, scurfin, results in the fatal lymphoproliferative disorder of the scurfy mouse. Nat Genet. 2001 Jan;27(1):68–73.

16. Sinicrope FA, Rego RL, Ansell SM, Knutson KL, Foster NR, Sargent DJ. Intraepithelial effector (CD3+)/regulatory (FoxP3+) T-cell ratio predicts a clinical outcome of human colon carcinoma. Gastroenterology. 2009 Oct;137(4):1270–9.

17. Vignali DAA, Collison LW, Workman CJ. How regulatory T cells work. Nat Rev Immunol. 2008 Jul;8(7):523–32.

18. Nakamura K, Kitani A, Strober W. Cell contact-dependent immunosuppression by CD4(+)CD25(+) regulatory T cells is mediated by cell surface-bound transforming growth factor beta. J Exp Med. 2001 Sep 3;194(5):629–44.

19. Grossman WJ, Verbsky JW, Tollefsen BL, Kemper C, Atkinson JP, Ley TJ. Differential expression of granzymes A and B in human cytotoxic lymphocyte subsets and T regulatory cells. Blood. 2004 Nov 1;104(9):2840–8.

20. Zhao DM, Thornton AM, DiPaolo RJ, Shevach EM. Activated CD4+CD25+ T cells selectively kill B lymphocytes. Blood. 2006 May 15;107(10):3925–32.

21. de la Rosa M, Rutz S, Dorninger H, Scheffold A. Interleukin-2 is essential for CD4+CD25+ regulatory T cell function. Eur J Immunol. 2004 Sep;34(9):2480–8.

22. Deaglio S, Dwyer KM, Gao W, Friedman D, Usheva A, Erat A, et al. Adenosine generation catalyzed by CD39 and CD73 expressed on regulatory T cells mediates immune suppression. J Exp Med. 2007 Jun 11;204(6):1257–65.

23. Sitkovsky MV, Ohta A. The "danger" sensors that STOP the immune response: the A2 adenosine receptors? Trends Immunol. 2005 Jun;26(6):299–304.

24. Tang Q, Adams JY, Tooley AJ, Bi M, Fife BT, Serra P, et al. Visualizing regulatory T cell control of autoimmune responses in nonobese diabetic mice. Nat Immunol. 2006 Jan;7(1):83–92.

25. Breed ER, Lee ST, Hogquist KA. Directing T cell fate: How thymic antigen presenting cells coordinate thymocyte selection. Semin Cell Dev Biol. 2018 Dec;84:2–10.

26. Walker LSK, Sansom DM. The emerging role of CTLA4 as a cell-extrinsic regulator of T cell responses. Nat Rev Immunol. 2011 Nov 25;11(12):852–63.

27. Aristin Revilla S, Kranenburg O, Coffer PJ. Colorectal Cancer-Infiltrating Regulatory T Cells: Functional Heterogeneity, Metabolic Adaptation, and Therapeutic Targeting. Front Immunol. 2022.

28. Mao X, Xu J, Wang W, Liang C, Hua J, Liu J, et al. Crosstalk between cancer-associated fibroblasts and immune cells in the tumor microenvironment: new findings and future perspectives. Mol Cancer. 2021 Oct 11;20(1):131.

29. Detmar M. Tumor angiogenesis. J Investig Dermatol Symp Proc. 2000 Dec;5(1):20–3.

30. World Health Organization (WHO). International Agency for Research on Cancer. World. In: GLOBOCAN 2020. WHO Website (2021). https://gco.iarc.fr/today/data/ factsheets/populations/900-world-fact-sheets.pdf\.

31. Jasperson KW, Tuohy TM, Neklason DW, Burt RW. Hereditary and familial colon cancer. Gastroenterology. 2010 Jun;138(6):2044–58.

32. Buccafusca G, Proserpio I, Tralongo AC, Rametta Giuliano S, Tralongo P. Early colorectal cancer: diagnosis, treatment and survivorship care. Crit Rev Oncol Hematol. 2019 Apr;136:20–30.

33. Colon Cancer Treatment. 2022. https://www.hopkinsmedicine.org/health/conditions-and-diseases/colon-cancer/colon-cancer-treatment

34. Qiu M, Hu J, Yang D, Cosgrove DP, Xu R. Pattern of distant metastases in colorectal cancer: a SEER based study. Oncotarget. 2015 Nov 17;6(36):38658–66.

35. Guinney J, Dienstmann R, Wang X, de Reyniès A, Schlicker A, Soneson C, et al. The consensus molecular subtypes of colorectal cancer. Nat Med. 2015 Nov;21(11):1350–6.

36. Hinshaw DC, Shevde LA. The Tumor Microenvironment Innately Modulates Cancer Progression. Cancer Res. 2019 Sep 15;79(18):4557–66.

37. Pelka K, Hofree M, Chen JH, Sarkizova S, Pirl JD, Jorgji V, et al. Spatially organized multicellular immune hubs in human colorectal cancer. Cell. 2021 Sep;184(18):4734-4752.e20.

38. Thanki K, Nicholls ME, Gajjar A, Senagore AJ, Qiu S, Szabo C, et al. Consensus Molecular Subtypes of Colorectal Cancer and their Clinical Implications. Int Biol Biomed J. 2017;3(3):105–11.

39. Roepman P, Schlicker A, Tabernero J, Majewski I, Tian S, Moreno V, et al. Colorectal cancer intrinsic subtypes predict chemotherapy benefit, deficient mismatch repair and epithelial-to-mesenchymal transition. Int J Cancer. 2014 Feb 1;134(3):552–62.

40. Everett E. Vokes MD, Edward Chu MD. Anti-EGFR Therapies: Clinical Experience in Colorectal, Lung, and Head and Neck Cancers. Oncology. 2006 Apr 29;20(5_Suppl_2).

41. Siveen KS, Prabhu K, Krishnankutty R, Kuttikrishnan S, Tsakou M, Alali FQ, et al. Vascular Endothelial Growth Factor (VEGF) Signaling in Tumour Vascularization: Potential and Challenges. Curr Vasc Pharmacol. 2017;15(4):339–51.

42. Loupakis F, Cremolini C, Masi G, Lonardi S, Zagonel V, Salvatore L, et al. Initial therapy with FOLFOXIRI and bevacizumab for metastatic colorectal cancer. N Engl J Med. 2014 Oct 23;371(17):1609–18.

43. Galon J, Costes A, Sanchez-Cabo F, Kirilovsky A, Mlecnik B, Lagorce-Pagès C, et al. Type, density, and location of immune cells within human colorectal tumors predict clinical outcome. Science. 2006 Sep 29;313(5795):1960–4.

44. Kryczek I, Wu K, Zhao E, Wei S, Vatan L, Szeliga W, et al. IL-17+ regulatory T cells in the microenvironments of chronic inflammation and cancer. J Immunol Baltim Md 1950. 2011 Apr 1;186(7):4388–95.

45. Xu J, Lamouille S, Derynck R. TGF-β-induced epithelial to mesenchymal transition. Cell Res. 2009 Feb;19(2):156–72.

46. Wang ZH, Peng WB, Zhang P, Yang XP, Zhou Q. Lactate in the tumour microenvironment: From immune modulation to therapy. EBioMedicine. 2021 Nov;73:103627.

47. Lu J, Liang Y, Meng H, Zhang A, Zhao J, Zhang C. Metabolic Controls on Epigenetic Reprogramming in Regulatory T Cells. Front Immunol. 2021;12:728783.

48. Multhoff G, Vaupel P. Lactate-avid regulatory T cells: metabolic plasticity controls immunosuppression in tumour microenvironment. Signal Transduct Target Ther. 2021 Apr 30;6(1):171.

49. Mj W, Pda V, Sj M, Ae OD, Rm P, S G, et al. Metabolic support of tumour-infiltrating regulatory T cells by lactic acid. Nature. 2021 Mar;591(7851).

50. Korbecki J, Grochans S, Gutowska I, Barczak K, Baranowska-Bosiacka I. CC Chemokines in a Tumor: A Review of Pro-Cancer and Anti-Cancer Properties of Receptors CCR5, CCR6, CCR7, CCR8, CCR9, and CCR10 Ligands. Int J Mol Sci. 2020 Oct 15;21(20):7619.

51. Zlotnik A, Yoshie O. Chemokines: a new classification system and their role in immunity. Immunity. 2000 Feb;12(2):121–7.

52. Cowan JE, McCarthy NI, Anderson G. CCR7 Controls Thymus Recirculation, but Not Production and Emigration, of Foxp3(+) T Cells. Cell Rep. 2016 Feb 9;14(5):1041–8.

53. Evans-Marin HL, Cao AT, Yao S, Chen F, He C, Liu H, et al. Unexpected Regulatory Role of CCR9 in Regulatory T Cell Development. PloS One. 2015;10(7):e0134100.

54. Smigiel KS, Richards E, Srivastava S, Thomas KR, Dudda JC, Klonowski KD, et al. CCR7 provides localized access to IL-2 and defines homeostatically distinct regulatory T cell subsets. J Exp Med. 2014 Jan 13;211(1):121–36.

55. Chanrion M, Kuperstein I, Barrière C, El Marjou F, Cohen D, Vignjevic D, et al. Concomitant Notch activation and p53 deletion trigger epithelial-to-mesenchymal transition and metastasis in mouse gut. Nat Commun. 2014 Oct 8;5:5005.

56. Haribhai D, Lin W, Relland LM, Truong N, Williams CB, Chatila TA. Regulatory T cells dynamically control the primary immune response to foreign antigen. J Immunol Baltim Md 1950. 2007 Mar 1;178(5):2961–72.

57. Lin W, Haribhai D, Relland LM, Truong N, Carlson MR, Williams CB, et al. Regulatory T cell development in the absence of functional Foxp3. Nat Immunol. 2007 Apr;8(4):359–68.

58. Pickup MW, Mouw JK, Weaver VM. The extracellular matrix modulates the hallmarks of cancer. EMBO Rep. 2014 Dec;15(12):1243–53.

59. Ling ZA, Zhang LJ, Ye ZH, Dang YW, Chen G, Li RL, et al. Immunohistochemical distribution of FOXP3+ regulatory T cells in colorectal cancer patients. Int J Clin Exp Pathol. 2018;11(4):1841–54.

60. Markert CL. Lactate dehydrogenase. Biochemistry and function of lactate dehydrogenase. Cell Biochem Funct. 1984;2(3):131–4.

61. Ziegler SF. FOXP3: of mice and men. Annu Rev Immunol. 2006;24:209–26.

62. Miyara M, Yoshioka Y, Kitoh A, Shima T, Wing K, Niwa A, et al. Functional Delineation and Differentiation Dynamics of Human CD4+ T Cells Expressing the FoxP3 Transcription Factor. Immunity. 2009 Jun 19;30(6):899–911.

63. Tran DQ, Ramsey H, Shevach EM. Induction of FOXP3 expression in naive human CD4+FOXP3 T cells by T-cell receptor stimulation is transforming growth factor-beta dependent but does not confer a regulatory phenotype. Blood. 2007 Oct 15;110(8):2983–90.

64. Bonnier F, Keating ME, Wróbel TP, Majzner K, Baranska M, Garcia-Munoz A, et al. Cell viability assessment using the Alamar blue assay: a comparison of 2D and 3D cell culture models. Toxicol Vitro Int J Publ Assoc BIBRA. 2015 Feb;29(1):124–31.

65. Xie BY, Wu AW. Organoid Culture of Isolated Cells from Patient-derived Tissues with Colorectal Cancer. Chin Med J (Engl). 2016 Oct 20;129(20):2469–75.

66. Herbertz S, Sawyer JS, Stauber AJ, Gueorguieva I, Driscoll KE, Estrem ST, et al. Clinical development of galunisertib (LY2157299 monohydrate), a small molecule inhibitor of transforming growth factor-beta signaling pathway. Drug Des Devel Ther. 2015;9:4479–99.

67. Tran DQ. In vitro suppression assay for functional assessment of human regulatory T cells. Methods Mol Biol Clifton NJ. 2013;979:199–212.

68. Brewer GJ, Torricelli JR, Evege EK, Price PJ. Optimized survival of hippocampal neurons in B27-supplemented Neurobasal, a new serum-free medium combination. J Neurosci Res. 1993 Aug 1;35(5):567–76.

69. Docea AO, Mitruţ P, Grigore D, Pirici D, Călina DC, Gofiţă E. Immunohistochemical expression of TGF beta (TGF-β), TGF beta receptor 1 (TGFBR1), and Ki67 in intestinal variant of gastric adenocarcinomas. Romanian J Morphol Embryol Rev Roum Morphol Embryol. 2012;53(3 Suppl):683–92.

70. Saito H, Tsujitani S, Oka S, Kondo A, Ikeguchi M, Maeta M, et al. The expression of transforming growth factor-β1 is significantly correlated with the expression of vascular endothelial growth factor and poor prognosis of patients with advanced gastric carcinoma. Cancer. 1999;86(8):1455–62.

71. Bejarano L, Jordão MJC, Joyce JA. Therapeutic Targeting of the Tumor Microenvironment. Cancer Discov. 2021 Apr 1;11(4):933–59.